AGH UNIVERSITY OF SCIENCE AND TECHNOLOGY

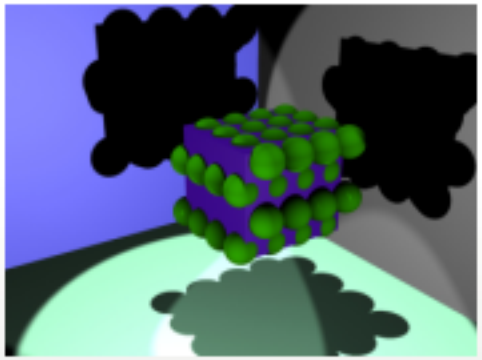

MODELLING POROSITY OF HIGH SURFACE AREA NANOPOWDERS OF THE GALLIUM NITRIDE GaN SEMICONDUCTOR

Jerzy F. Janik,* Mariusz Drygas, L. Czepirski

AGH University of Science and Technology, Faculty of Energy and Fuels
Al. Mickiewicza 30, 30 059 Krakow, Poland

**E-mail*: janikj@agh.edu.pl

IVC18/ICN+T2010/ICSS-14/VASSCAA-5, Beijing, China, 2010

Gallium nitride GaN

- two crystallographic forms at RT:
  - wurzite (hexagonal): a = 3.168 Å and c = 5.178 Å
  - zinc blende (cubic): a = 4.51 Å
- thermal stability up to 1000 °C
- high chemical stability
- strong piezoelectric effect
- wide bandgap semiconductor: 3.4 eV (hexagonal)
- alloys with InN and AlN; alloy bandgap range: 1.8–6.2 eV
- GaN bandgap is a function of particle size for R < 11 nm

Materials forms of GaN

Gallium nitride GaN

Microcrystals

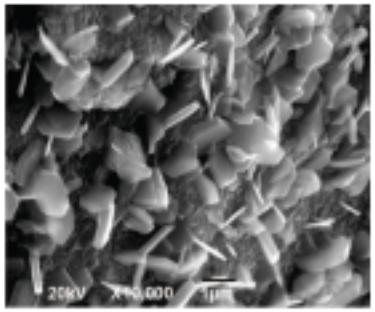

L. Lei, D. He; *Cryst. Growth Des.*, 2009, *9*, 1263.

Bulk crystals

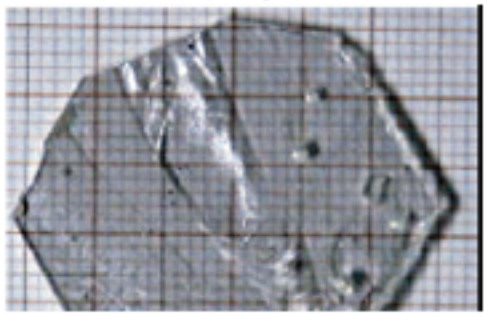

T. Fukuda, D. Ehrentraut; *J. Cryst. Growth*, 2007, *305*, 304.

Thin films

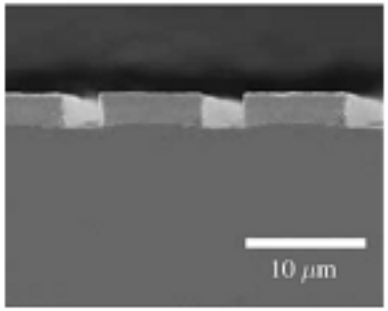

H. K. Cho *et al.*; *Superlattices and Microstruct.*, 2004, *36*, 385.

Quantum dots

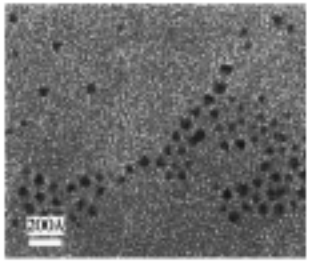

O. I. Micic *et al.*, *Appl. Phys. Lett.*, 1999, *75*, 4.

Porous surface

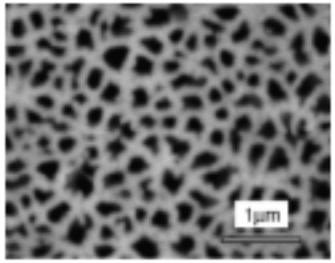

F. K. Yam, Z. Hassan, S. S. Ng; *Thin Solid Films*, 2007, *515*, 3469.

Nanopowders

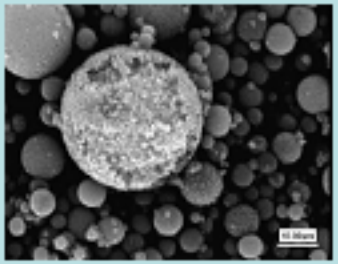

J. F. Jan *et al.*; *J. Phys. Chem. Solids*, 2004, *65*, 639.

Nanotubes Nanofibers

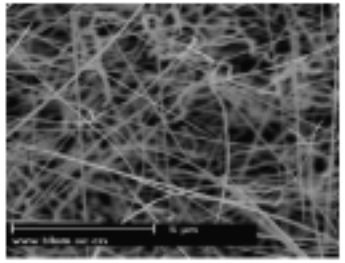

W. Lu *et al.*; *J. Cryst. Growth*, 2007, 307, 1.

Porous GaN

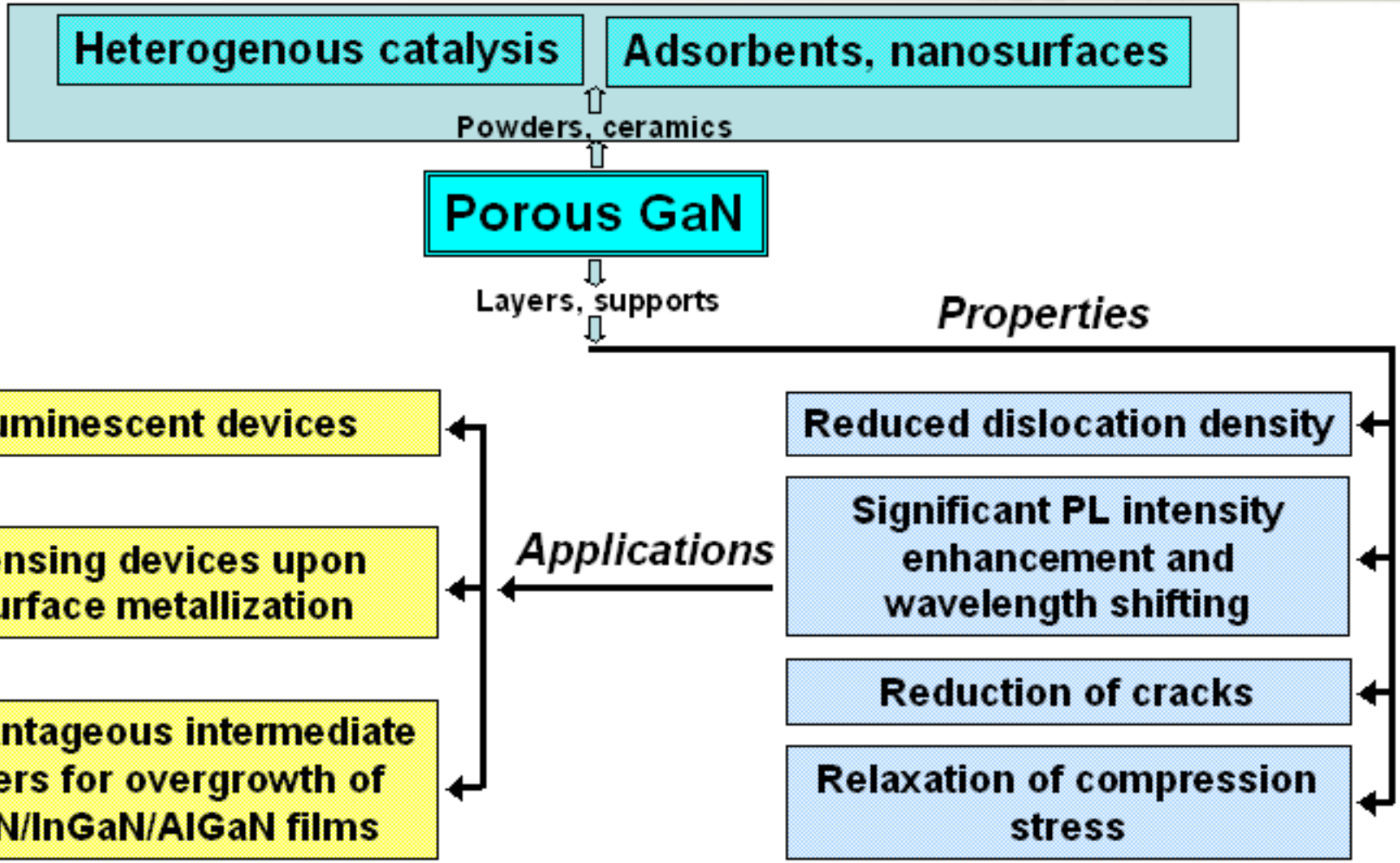
Heterogenous catalysis
Adsorbents, nanosurfaces
Powders, ceramics
Porous GaN
Layers, supports
Properties
Luminescent devices
Sensing devices upon surface metallization
Advantageous intermediate layers for overgrowth of GaN/InGaN/AlGaN films
Applications
Reduced dislocation density
Significant PL intensity enhancement and wavelength shifting
Reduction of cracks
Relaxation of compression stress

This work – anaerobic synthesis of GaN nanopowders

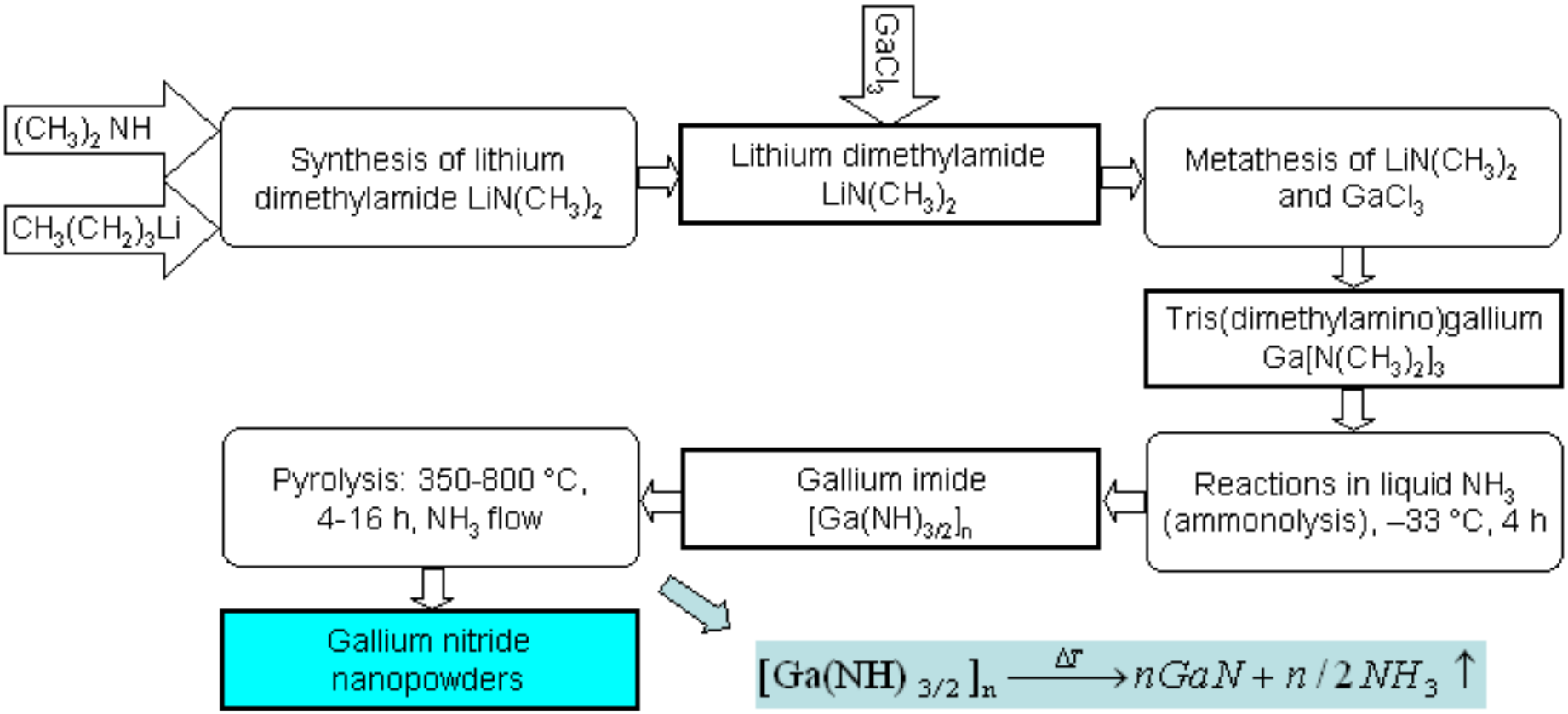

[1] J. F. Janik, R. L. Wells; *Chem. Mater.* **1996,** *8*, 2708.
[2] J. F. Janik, R. L. Wells, J. L. Coffer, J. V. St. John, W. T. Pennington, G. L. Schimek; *Chem. Mater.* **1998,** *10*, 1613.

This work – *aerosol* synthesis of GaN nanopowders

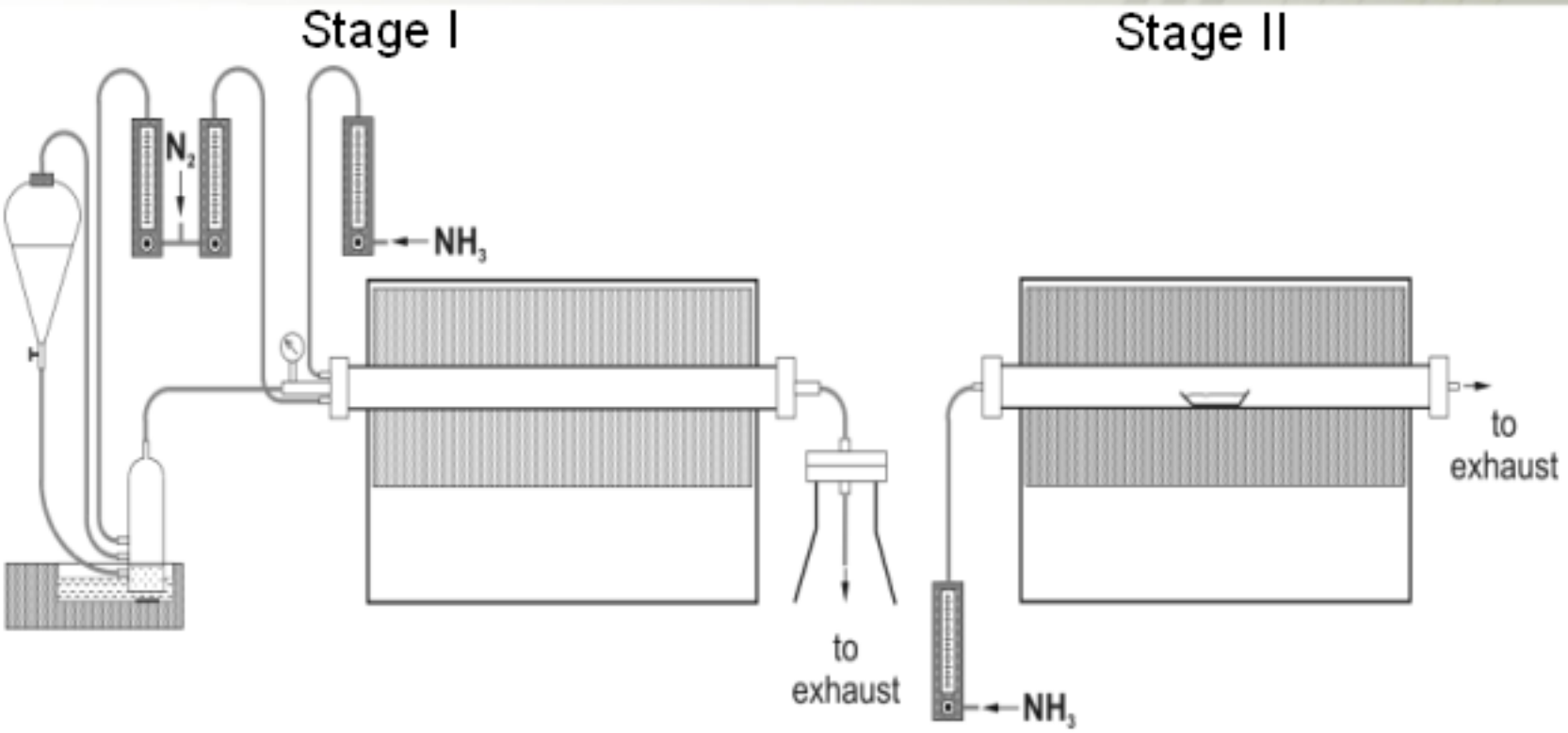

$$2Ga(NO_3)_3 \xrightarrow{1050\,^{\circ}C} Ga_2O_3 + "3N_2O_5"\uparrow \cdots Ga_2O_3 + 2NH_3 \xrightarrow{950\text{-}975\,^{\circ}C} 2GaN + 3H_2O\uparrow$$

[1] E. A. Pruss, G. L. Wood, W. J. Kroenke, R. T. Paine; *Chem. Mater.* **2000**, *12*, 19.
[2] J. F. Janik, M. Drygas, S. Stelmakh, E. Grzanka, B. Palosz, R. T. Paine; *phys. stat. sol. a* **2006**, *203*, 1301.

This work – synthesis of GaN nanopowders from Ga_2O_3

Reaction of bulk gallium oxide powder with ammonia

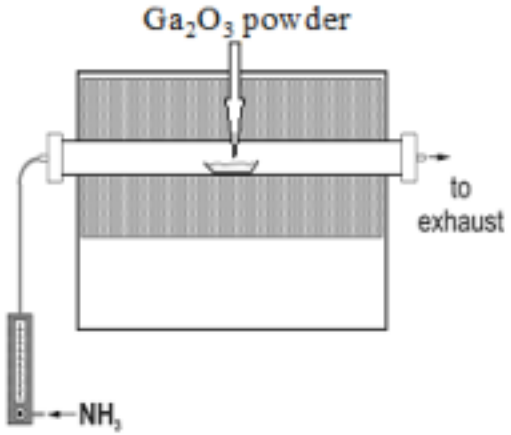

$$Ga_2O_3 + 2NH_3 \xrightarrow{950\,^{\circ}C} 2GaN + 3H_2O\uparrow$$

J. F. Janik, M. Drygas, S. Stelmakh, E. Grzanka, B. Palosz, R. T. Paine; *phys. stat. sol. a* **2006**, *203*, 1301.

High surface area GaN powders – to date

"Adsorption characteristics of powders of nanometric gallium nitride and aluminium nitride" - L. Czepirski, J. F. Janik, E. Komorowska-Czepirska, R. L. Wells; *Adsorpt. Sci. Technol.* **2002**, 20 (8), 723.

⇩

Max. BET surface area: 224 m^2/g

"Template assisted design of microporous gallium nitride materials" – G. Chaplais, K. Schlichte, O. Stark, R. A. Fischer, S. Kaskel; *Chem. Comm.* **2003**, 730.

⇩

Max. BET surface area: 320 m^2/g

" Porosity control in pre-ceramic molecular precursor-derived GaN based materials" – G. Chaplais, S. Kaskel; *J. Mater. Chem.* **2004**, 14, 1017.

⇩

Max. BET surface area: 331 m^2/g

Capillary condensation *vs.* pore size and spherical particle morphology

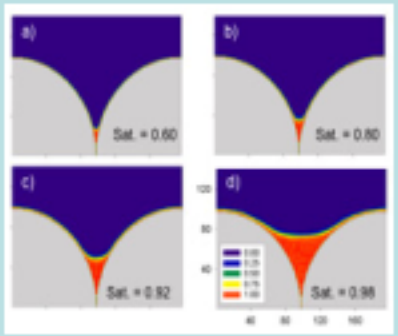

Liquid meniscus formation between spherical particles
Seonmin Kim, Univ. of Maryland, USA

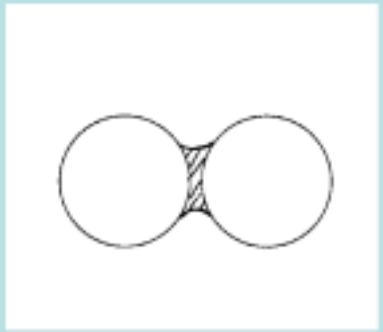

Bridging between two spheres due to capillary condensation

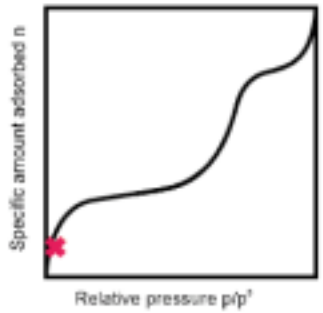

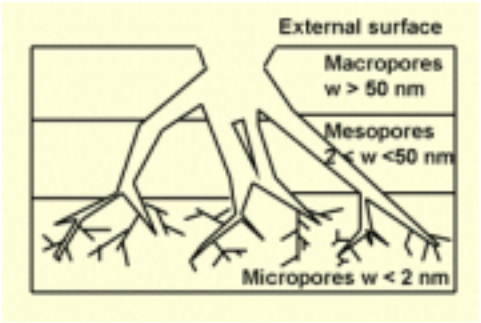

Dr. Nishith Verma, Kanpur, India

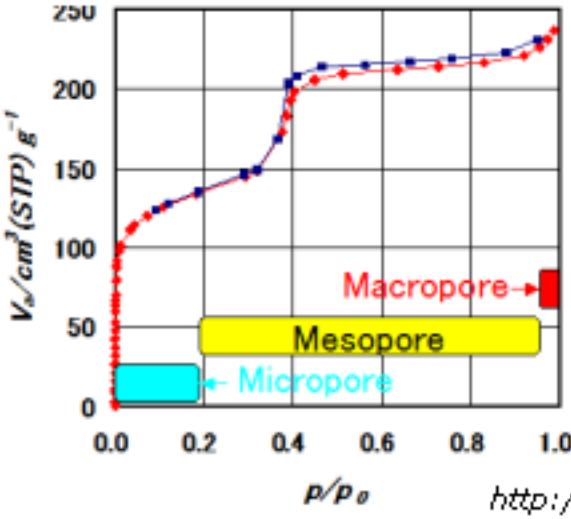

If a capillary's radius increases sharply, then capillary condensation (adsorption) will cease until an equilibrium vapor pressure is reached which satisfies the larger pore radius. However, during evaporation (desorption), liquid will remain filled to the larger pore radius until an equilibrium vapor pressure that satisfies the smaller pore radius is reached.

http://www.nippon-bel.co.jp/tech/seminar12_e.html

[1] D. Dollimore, D., G. R. Heal; *J. Colloid Interf. Sci.* **1973**, *42(2)*, 233.
[2] D. C. Howard, R. Wilson; *J. Colloid Interf. Sci.* **1976**, *57(2)*, 276.

Langmuir theory

Assumptions of Langmuir theory

http://upload.wikimedia.org/wikipedia/commons/0/0b/Langmuir_izoterma.png

1. Fixed number of adsorption sites are available on the surface.
2. All the vacant sites are of equal size and shape on the surface.
3. Each site can hold maximum of one gaseous molecule and a constant amount of heat energy is released during this process.
4. Dynamic equilibrium exists between adsorbed gaseous molecules and the free gaseous molecules.

$$A(g) + B(s) \underset{\text{desorption}}{\overset{\text{adsorption}}{\rightleftharpoons}} AB$$

5. Adsorption is monolayer.

Brunauer, Emmett, Teller (BET) theory

Assumptions of BET theory

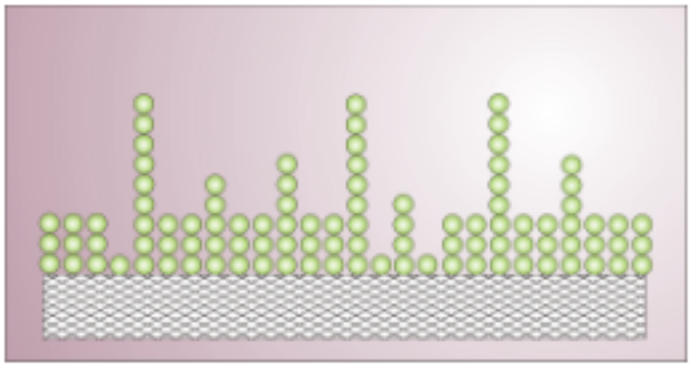

http://upload.wikimedia.org/wikipedia/commons/8/83/BET_Multilayer_Adsorption.jpg

The concept of the theory is an extension of the Langmuir theory, which is a theory for monolayer molecular adsorption, to multilayer adsorption with the following hypotheses.

1. Gas molecules physically adsorb on the surface with random distribution of sites covered by one, two, three, etc. molecules.
2. There is no interaction between each adsorption layer.
3. The Langmuir theory can be applied to each layer.

Barrett, Joyner, Halenda (BJH) theory

Assumptions of BJH theory

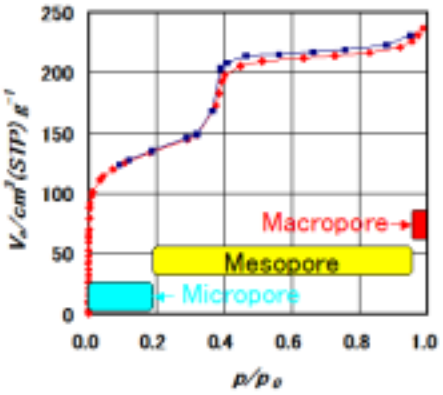

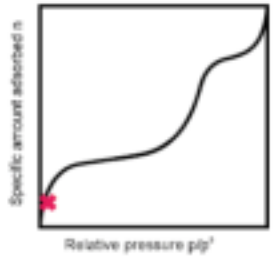

1. The relative pressure p/p_o at which decondensation (from capillary phase to multilayer adsorbed phase) occurs in a cylindrical pore is given by the Kelvin law,

$$kTln(p/p_o) = -2\,\sigma\,v_1/(R-t)$$

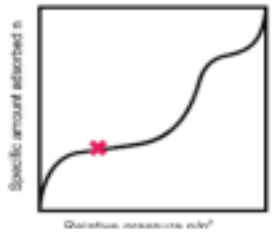

k – Boltzmann constant, T – temperature, p – equilibrium pressure, p_o – saturation vapor pressure, σ – surface tension, v_1 – liquid molecular volume, R – pore radius, t – multilayer thickness

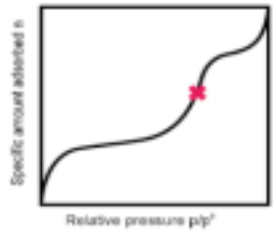

2. The curvature of the solid surface has no influence on *t*. Thus, *t* can be experimentally determined using non porous adsorbents.

$$kTln(p/p_o) = U(t)$$

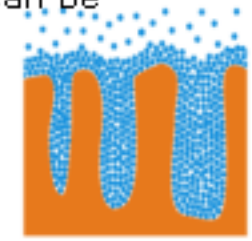

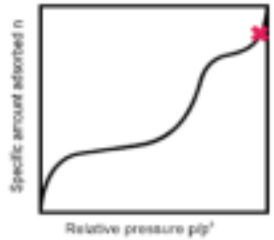

Samples and experimental results

No.	Sample	D_{GaN} (XRD) [nm]	d_{He} [g/cm^3]	S_{BET} [m^2/g]	S_{Lang} [m^2/g]	S_{meso} (BJH/des) [m^2/g]	V_{meso} (BJH/des) [cm^3/g]	Av. pore size (BJH/des) [nm]
1	Anaer 450 vac	1.0	3.6	179	265	30.2	0.021	2.7
2	Anaer 450 N_2	1.2	3.8	165	262	145	0.089	2.4
3	Anaer_350_NH_3	1.6	4.0	134	216	96	0.070	3.7
4	Anaer_450_NH_3	1.8	4.5	**222**	**357**	**216**	0.138	2.6
5	Anaer_600_NH_3	3.0	5.2	103	162	133	0.154	4.6
6	Anaer 700 NH_3	6.0	5.2	58	91	76	0.146	6.9
7	Anaer 800 NH_3	8.1	5.0	42	66	66	0.143	17.8
8	Aero D/M 950	17.0	6.0	23.5	37.0	38.0	0.181	19.0
9	Aero_DMF_950	18.0	6.0	24.0	37.5	42.0	**0.213**	**20.3**
10	Aero_MeOH_950	18.0	6.1	20.8	32.1	22.8	0.086	15.1
11	Aero_H_2O_975	30.0	6.0	6.3	9.7	5.2	0.015	11.5
12	Ga_2O_3 950	39.0	6.1	8.0	12.2	6.7	0.019	11.6

Adsorption isotherms (N_2, 77.5 K) and mesopore distribution (BJH) - 1

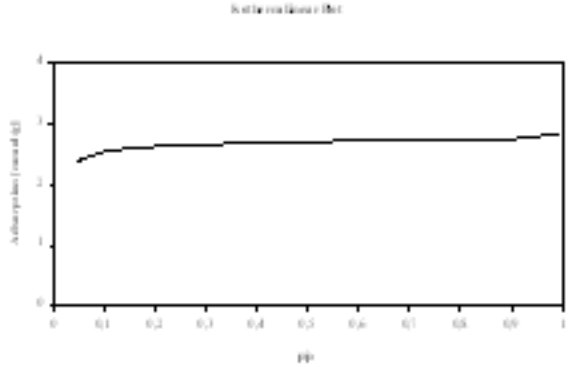

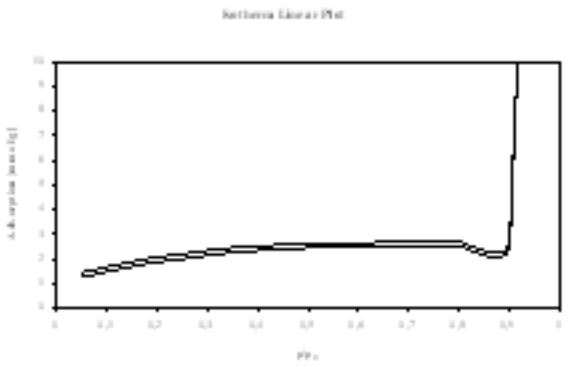

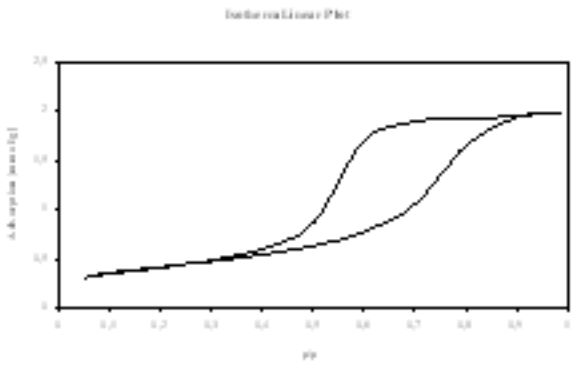

Anaero_450_vac

Anaero_450_N_2

Anaero_350_NH_3

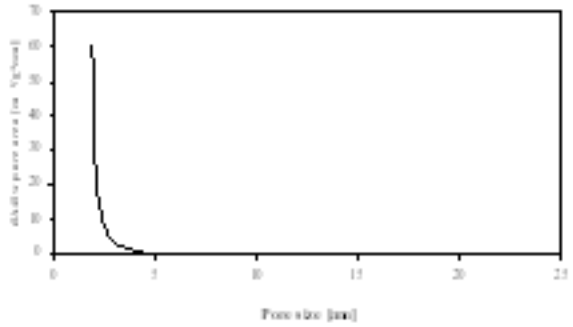

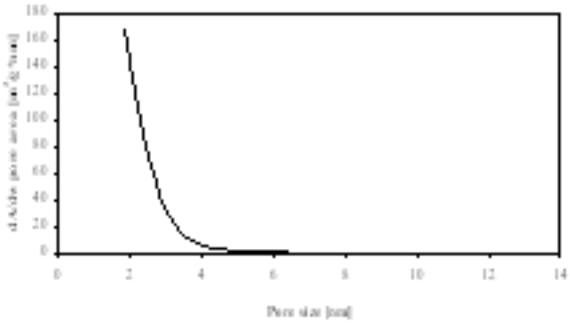

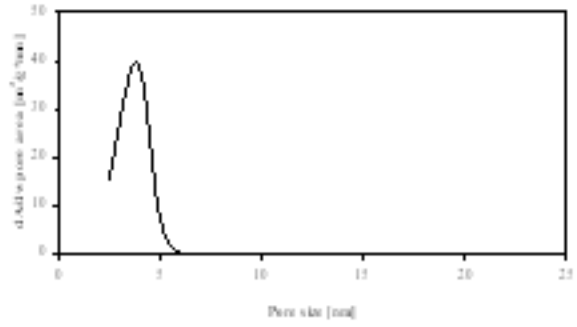

Adsorption isotherms (N_2, 77.5 K) and mesopore distribution (BJH) - 2

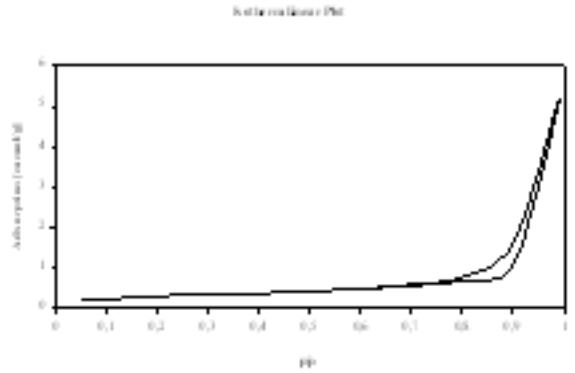

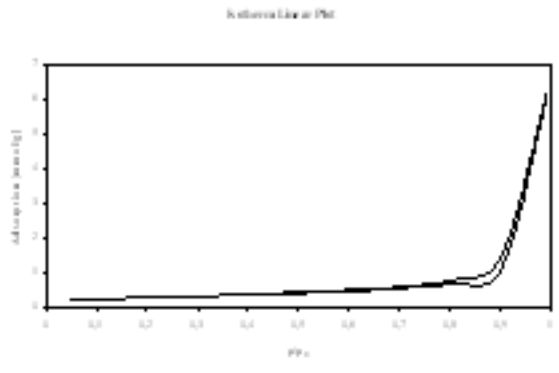

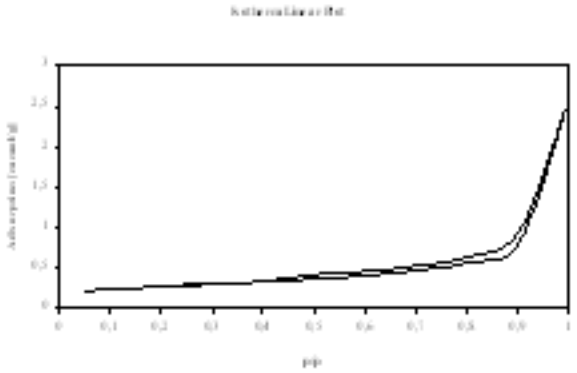

Aero_DMF/MeOH_950

Aero_DMF_950

Aero_MeOH_950

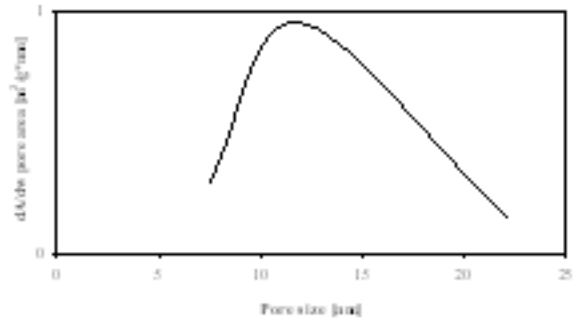

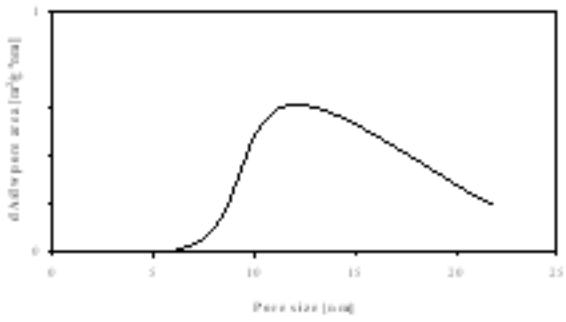

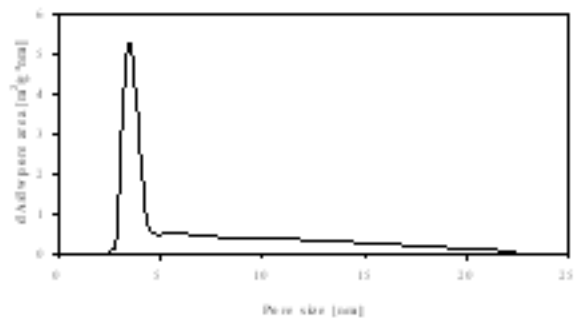

XRD size determination aspect

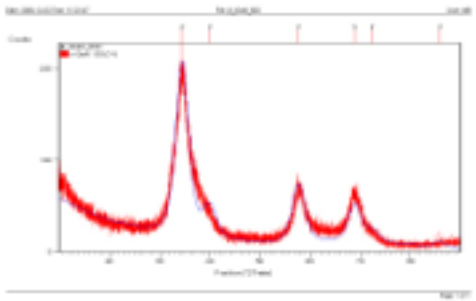

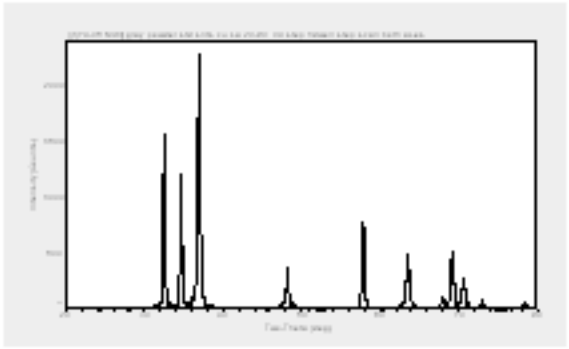

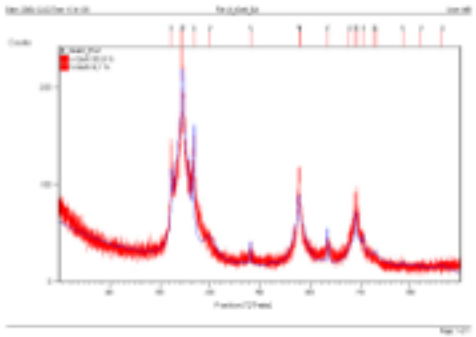

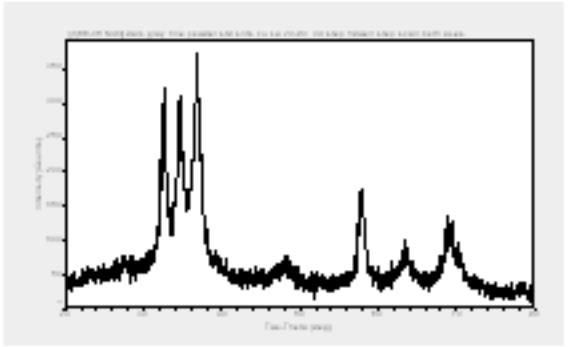

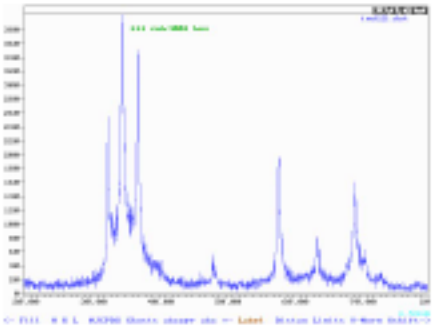

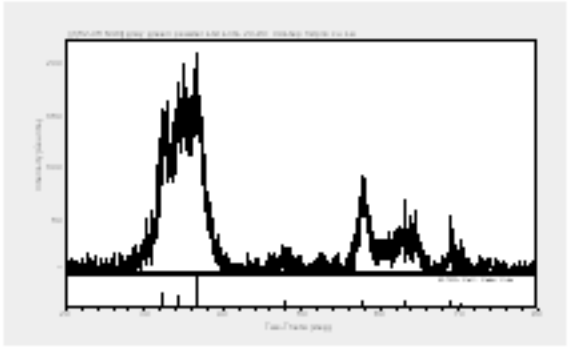

Scherrer's equation:

Av. crystallite size = K·λ/B·cosΘ

K (crystallite shape factor) = 0.9 (usually)
λ (X-ray wavelength) = 1.540598 Å (Cu K_α)
B (line broadening at half the maximum) = sq. root ($B_{obs.}^2$ - $B_{std.}^2$)
Θ (Bragg angle)

- possible superimposed peaks for the hexagonal and cubic polytypes
- potentially defected hexagonal polytype
- vaquely addressed problem of lattice strain contribution to line broadening in nanograins
- equivocal interpretation of X-ray diffraction outcome for small nanocrystallites due to significant contribution of surface layers

⇩

Increased uncertainty in average size determinations for D < *ca.* 10 nm

TEM pictures of GaN powders

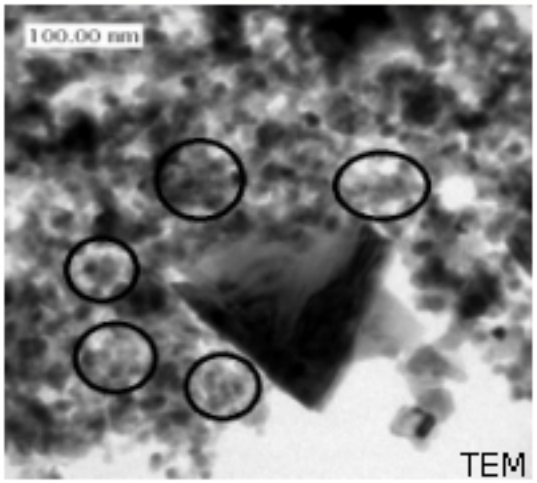

Anaero - 900 ºC, 4 h; D_{av} =15 nm

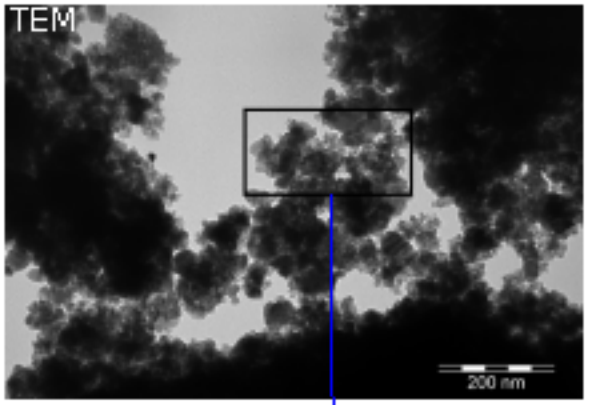

Anaero_600_NH_3; D_{av} = 3.0 nm

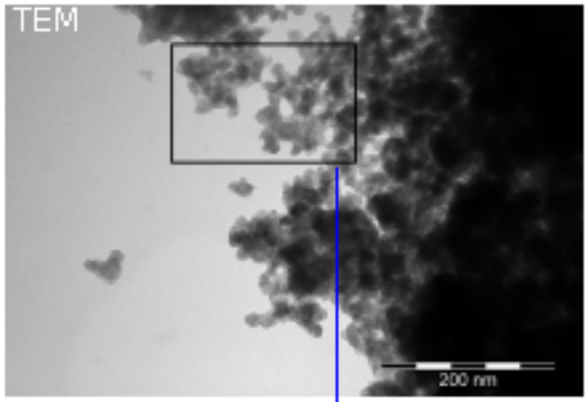

Anaero_800_NH_3; D_{av} = 8.1 nm

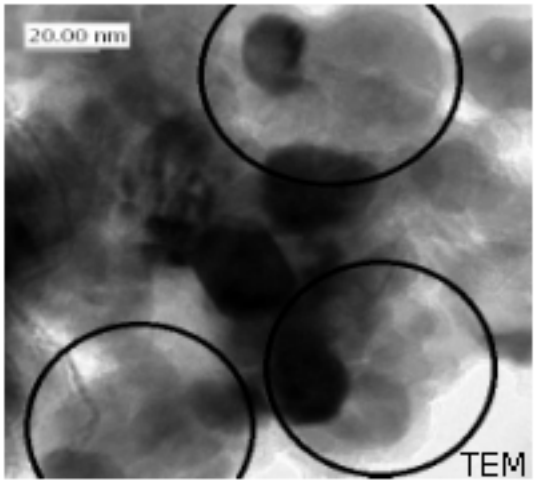

Aero - 975 ºC, 6 h; D_{av} = 20 nm

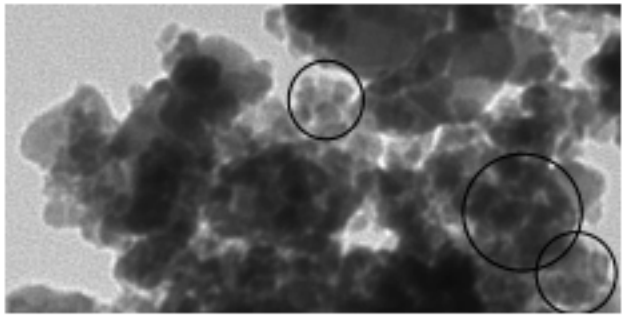

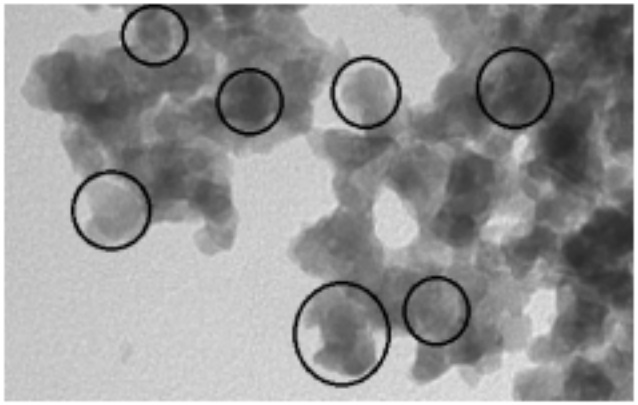

SEM pictures of GaN powders

Aerosol-assisted synthesis, 950-975 ^{o}C, 6 h

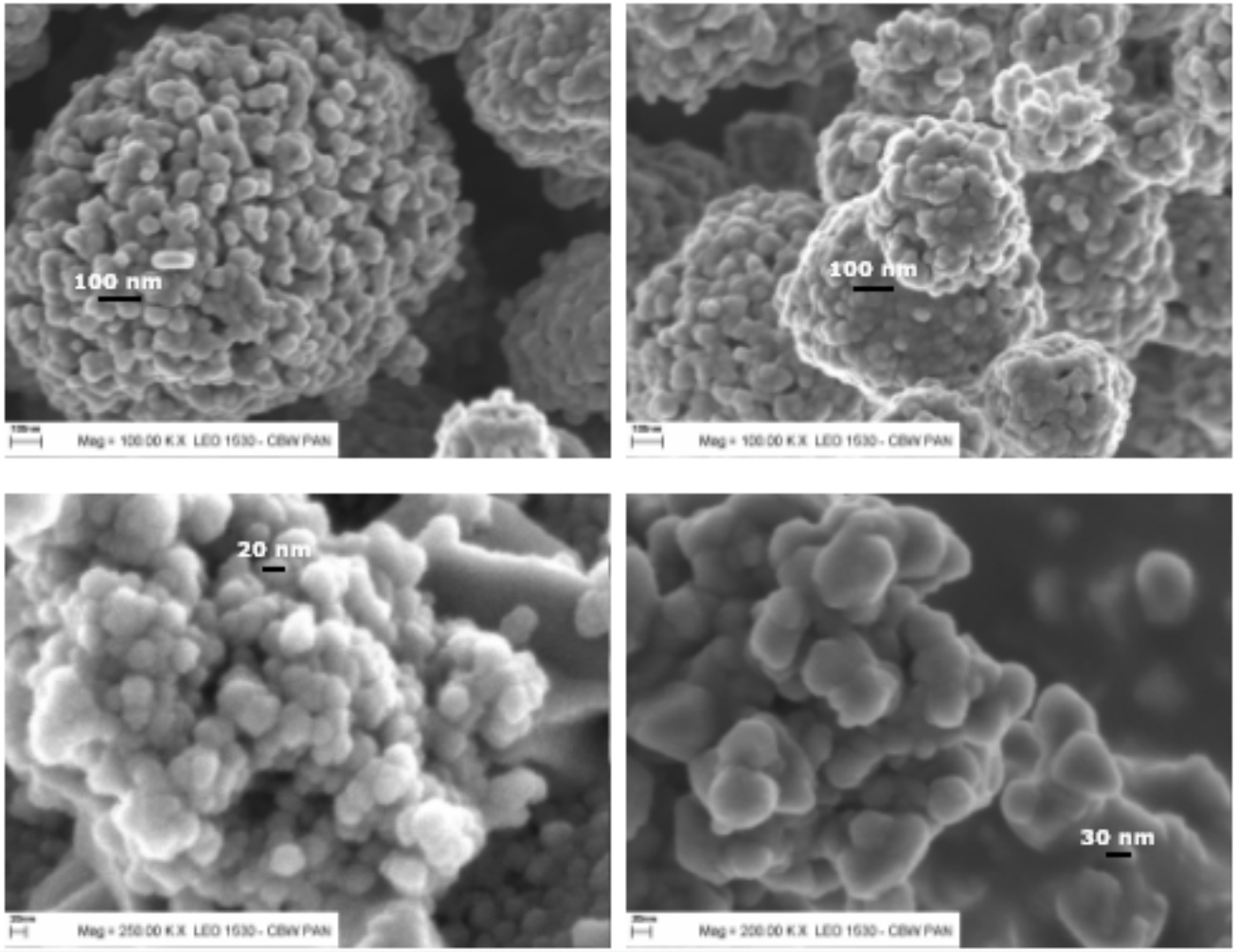

"Porosity" model ramifications – phenomenological approach

Can pore system and pore surface area for gallium nitride GaN nanopowders be adequately modelled by interparticle spaces and surface area, respectively, of closely packed equiradial spherical particles as the simplest model case?

Model validation **by testing correlation between the experimental standard "porosity" parameters, *i.e.*, BET, Langmuir, and BJH-derived specific surface areas and the experimental "particle size" parameter, *i.e.*, average crystallite diameter from XRD determinations with respect to predictions of the model.**

Helium density aspect

$$d_{aggl}\ [g/cm^3] = \frac{m_{aggl}}{V_{aggl}} = 6.1 \cdot \frac{n \cdot \frac{4}{3}\pi(\frac{D_{GaN}}{2})^3}{n \cdot \frac{4}{3}\pi(\frac{D_{GaN}+D_{He}}{2})^3} = 6.1 \cdot \frac{D_{GaN}^{\ 3}}{(D_{GaN}+D_{He})^3} = \boxed{6.1 \cdot \frac{D_{GaN}^{\ 3}}{(D_{GaN}+0.26)^3}}$$

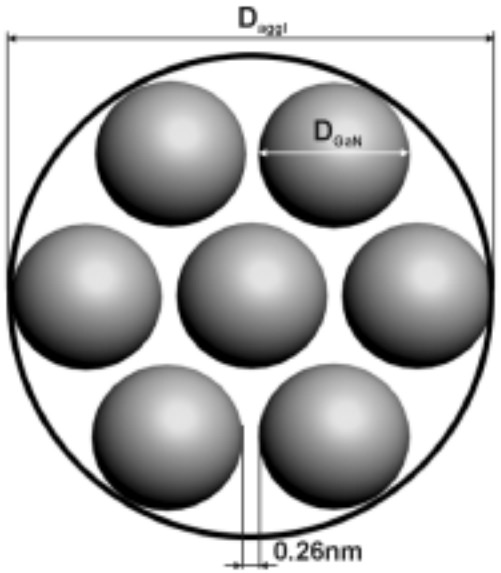

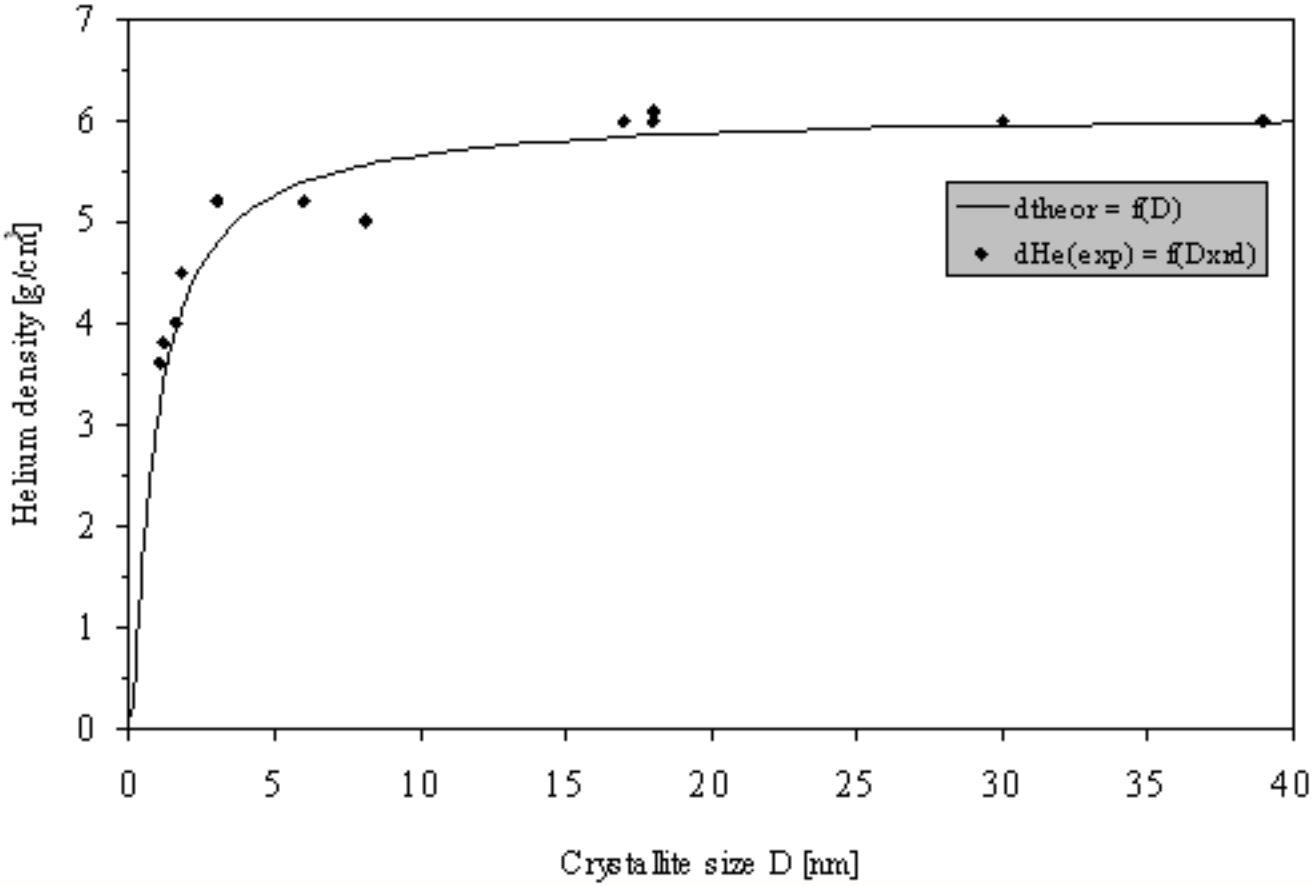

Model 1 – double adsorbate layer particle bridging

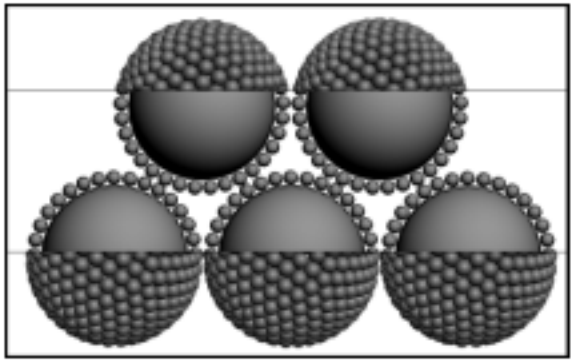

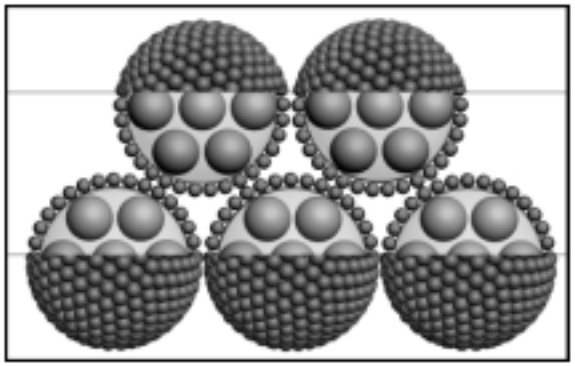

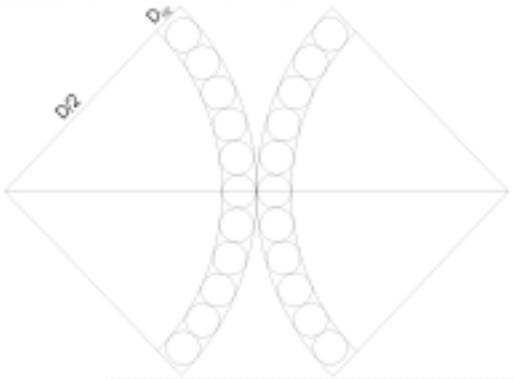

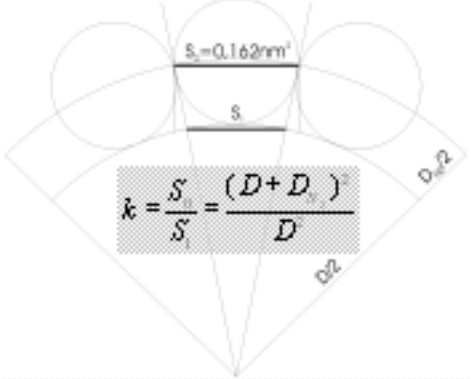

$$n/cm^3 = \frac{0.7405}{\frac{4}{3}\pi(\frac{D+2D_{N_2}}{2})^3 \cdot 10^{-21}}$$; n - number of particles per 1 cm³

$$S_p\,[m^2] = 4\pi(\frac{D}{2})^2 \cdot 10^{-18}$$; S_p - particle surface area

$$S\,[m^2/cm^3] = n \cdot S_p = \frac{0.7405}{\frac{4}{3}\pi(\frac{D+2D_{N_2}}{2})^3 \cdot 10^{-21}} \cdot 4\pi(\frac{D}{2})^2 \cdot 10^{-18} = \frac{4443 \cdot D^2}{(D+2D_{N_2})^3}$$

$$S\,[m^2/g] = \frac{4443 \cdot D^2}{(D+2D_{N_2})^3} \cdot \frac{(D+D_{He})^3}{6.1 \cdot D^3} = \frac{728.36 \cdot D^2}{(D+2D_{N_2})^3} \cdot \frac{(D+D_{He})^3}{D^3}$$

D – particle (crystallite/agglomerate) diameter [nm]
D_{He} = 0.260 nm – helium atom kinetic diameter
D_{N_2} = 0.455 nm – nitrogen molecule diameter

$$S_{corr}\,[m^2/g] = S\,[m^2/g] \cdot k = \frac{728.36 \cdot (D+D_{N_2})^2}{(D+2D_{N_2})^3} \cdot \frac{(D+D_{He})^3}{D^3}$$

Model 1 – double adsorbate layer particle bridging

Model 1 - theoretical relationships between the specific surface and sphere diameter

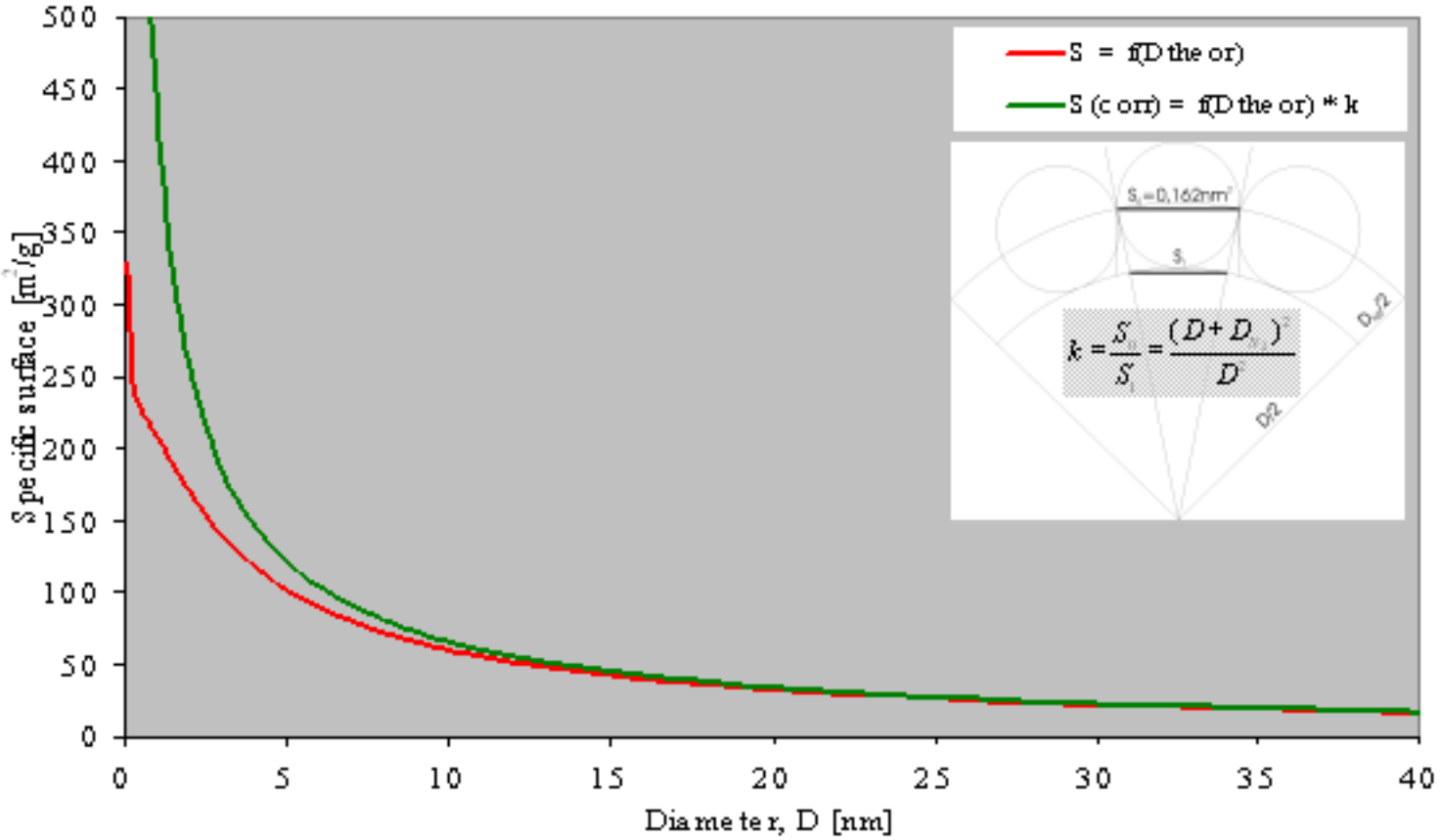

Model 2 – single adsorbate layer particle bridging

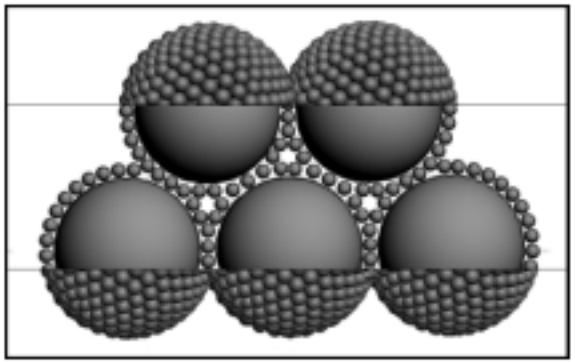

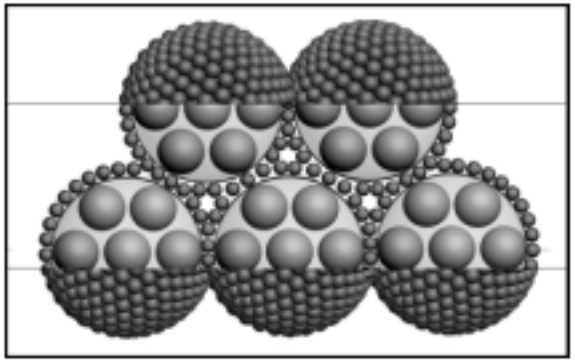

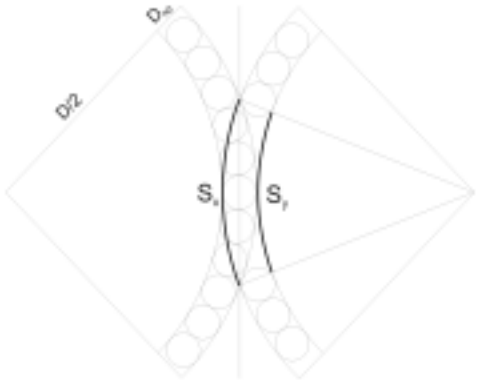

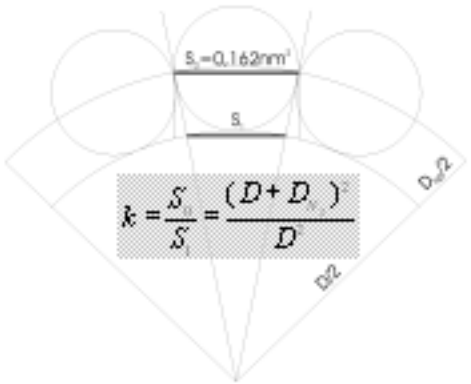

D – particle (crystallite/agglomerate) diameter [nm]
D_{He} = 0.260 nm – helium kinetic diameter
D_{N2} = 0.455 nm – nitrogen molecule diameter

$$S\,[m^2/g] = \left(D^2 - \frac{3\cdot D^2\cdot D_{N_2}}{D+2D_{N_2}}\right)\cdot\frac{728.36}{(D+D_{N_2})^3}\cdot\frac{(D+D_{He})^3}{D^3}$$

$$S_{corr}\,[m^2/g] = S\,[m^2/g]\cdot k = \left(1-\frac{3\cdot D_{N_2}}{D+2D_{N_2}}\right)\cdot\frac{728.36}{(D+D_{N_2})}\cdot\frac{(D+D_{He})^3}{D^3}$$

Model 2 – single adsorbate layer particle bridging

Model 2 - theoretical relationships between the specific surface and sphere diameter

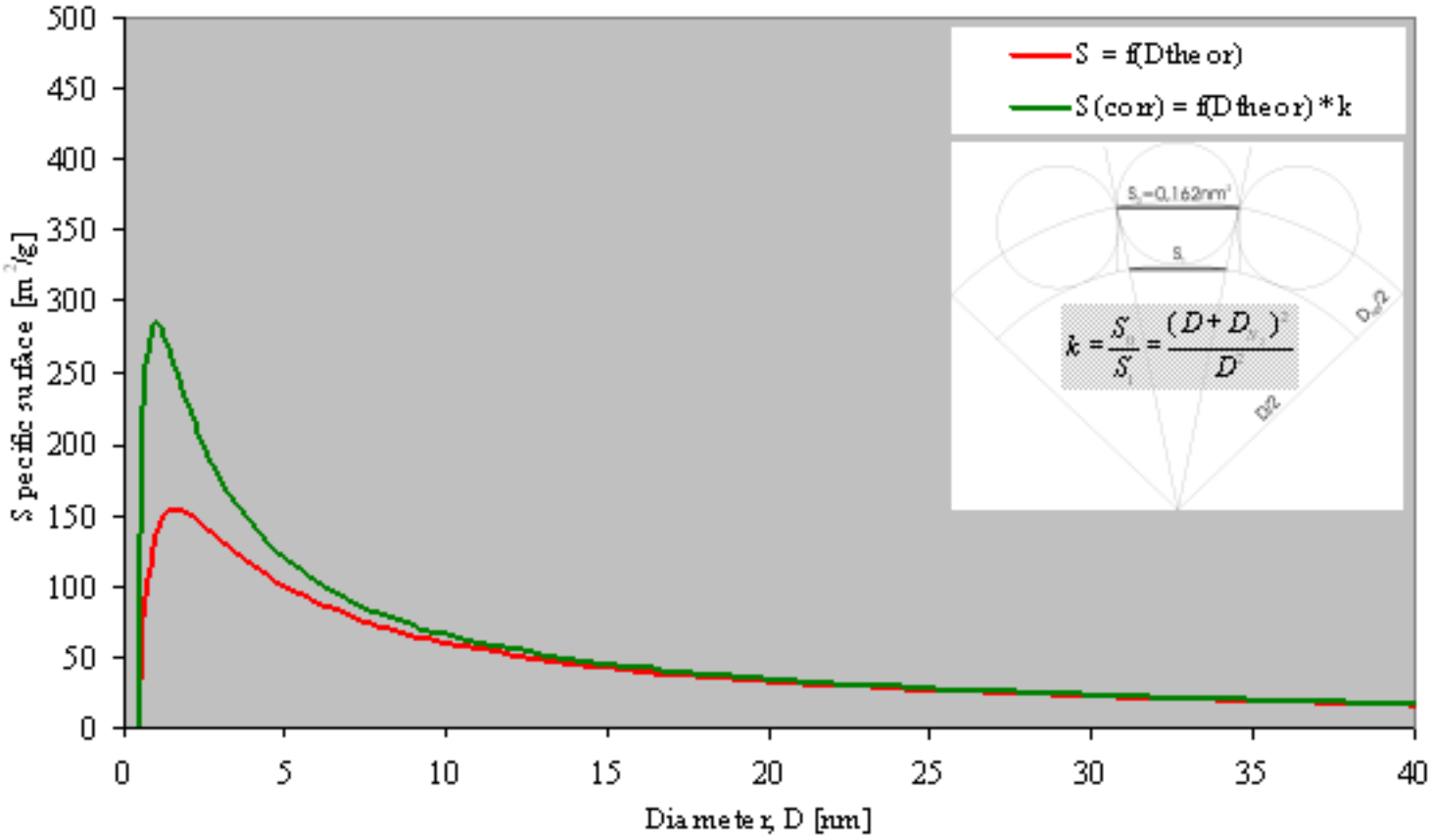

Model 3 – no adsorbate layer particle bridging

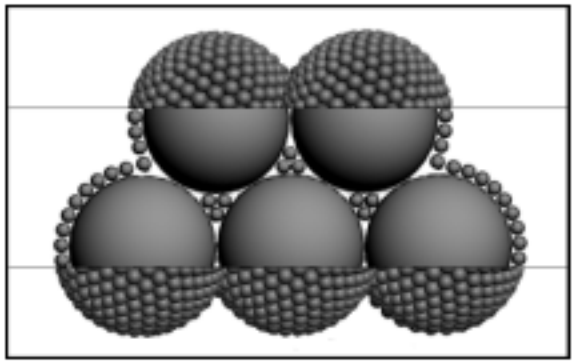

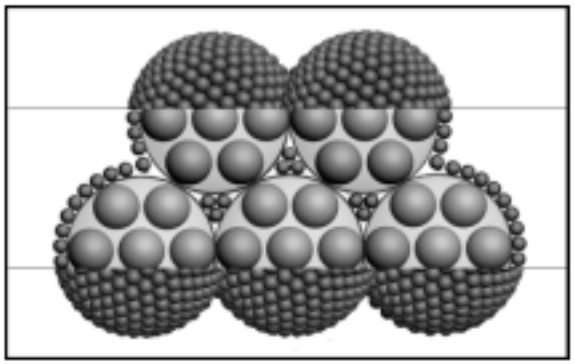

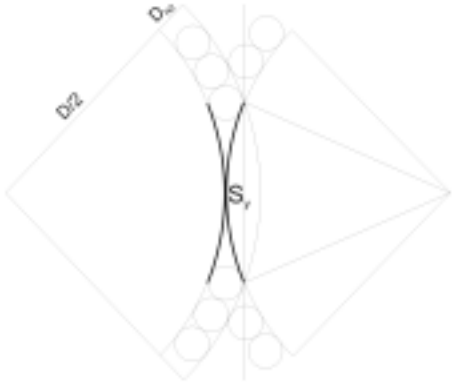

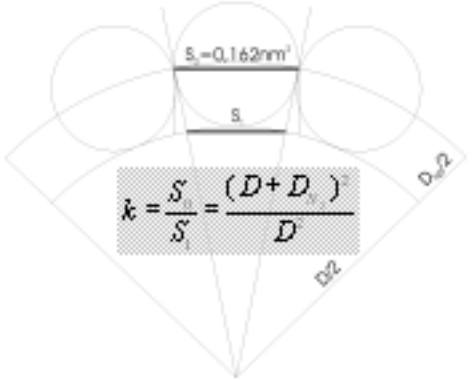

D – particle (crystallite/agglomerate) diameter [nm]
D_{He} = 0.260 nm – helium kinetic diameter
D_{N2} = 0.455 nm – nitrogen molecule diameter

$$S\,[m^2/g] = \left(1 - \frac{6D_{N_2}}{D + 2D_{N_2}}\right) \cdot \frac{728.36}{D} \cdot \frac{(D + D_{He})^3}{D^3}$$

$$S_{corr}\,[m^2/g] = S\,[m^2/g] \cdot k = \left(1 - \frac{6D_{N_2}}{D + 2D_{N_2}}\right) \cdot \frac{728.36 \cdot (D + D_{N_2})^2}{D^3} \cdot \frac{(D + D_{He})^3}{D^3}$$

Model 3 – no adsorbate layer particle bridging

Model 3 - theoretical relationships between the specific surface and sphere diameter

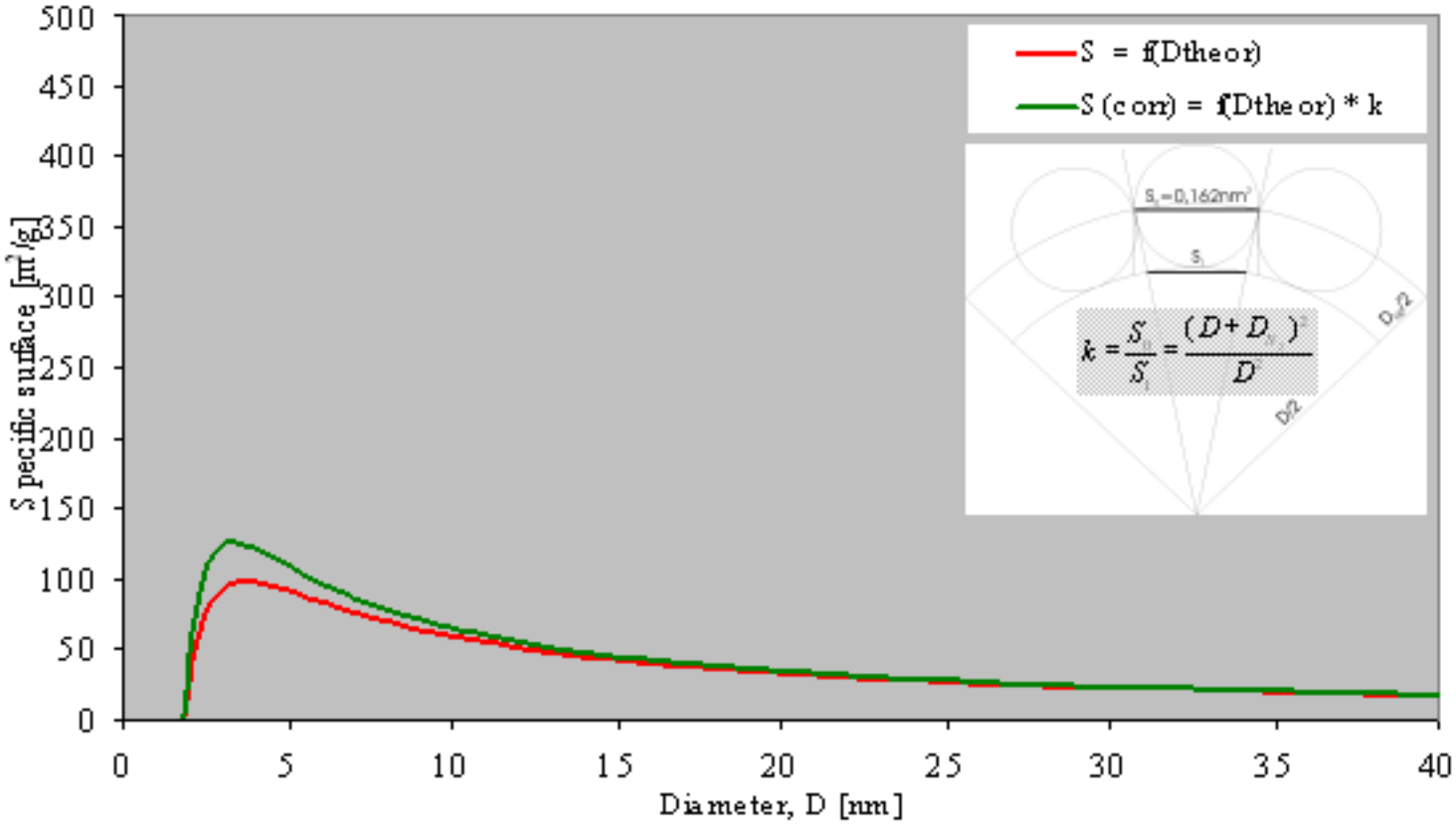

Model 1 – correlation equations

(i) *No correction* for the cross-sectional area of N_2

$$S\,[m^2/g] = \frac{728.36 \cdot D^2}{(D + 2D_{N_2})^3} \cdot \frac{(D + D_{He})^3}{D^3}$$

a – relaxed variable
(relaxed D)

$$S\,[m^2/g] = \frac{728.36 \cdot (a \cdot D)^2}{(a \cdot D + 2D_{N_2})^3} \cdot \frac{(D + D_{He})^3}{D^3}$$

a, b – relaxed variables
(relaxed D and "constant")

$$S\,[m^2/g] = \frac{b \cdot (a \cdot D)^2}{(a \cdot D + 2D_{N_2})^3} \cdot \frac{(D + D_{He})^3}{D^3}$$

(ii) *Corrected* for the cross-sectional area of N_2

$$S\,[m^2/g] = \frac{728.36 \cdot (D + D_{N_2})^2}{(D + 2D_{N_2})^3 \cdot} \cdot \frac{(D + D_{He})^3}{D^3}$$

a – relaxed variable
(relaxed D)

$$S_{corr}\,[m^2/g] = \frac{728.36 \cdot (a \cdot D + D_{N_2})^2}{(a \cdot D + 2D_{N_2})^3} \cdot \frac{(D + D_{He})^3}{D^3}$$

a, b – relaxed variables
(relaxed D and "constant")

$$S_{corr}\,[m^2/g] = \frac{b \cdot (a \cdot D + D_{N_2})^2}{(a \cdot D + 2D_{N_2})^3} \cdot \frac{(D + D_{He})^3}{D^3}$$

Model 2 – correlation equations

(i) *No correction* for the cross-sectional area of N_2

$$S\,[m^2/g] = \left(D^2 - \frac{3\cdot D^2\cdot D_{N_2}}{D+2D_{N_2}}\right)\cdot\frac{728.36}{(D+D_{N_2})^3}\cdot\frac{(D+D_{He})^3}{D^3}$$

a – relaxed variable
(relaxed D)

$$S\,[m^2/g] = \left((a\cdot D)^2 - \frac{3\cdot D^2\cdot D_{N_2}}{a\cdot D+2D_{N_2}}\right)\cdot\frac{728.36}{(a\cdot D+D_{N_2})^3}\cdot\frac{(D+D_{He})^3}{D^3}$$

a, b – relaxed variables
(relaxed D and one "constant")

$$S\,[m^2/g] = \left((a\cdot D)^2 - \frac{3\cdot D^2\cdot D_{N_2}}{a\cdot D+2D_{N_2}}\right)\cdot\frac{b}{(a\cdot D+D_{N_2})^3}\cdot\frac{(D+D_{He})^3}{D^3}$$

a, b, c – relaxed variables
(relaxed D and two "constants")

$$S\,[m^2/g] = \left((a\cdot D)^2 - \frac{c\cdot D^2\cdot D_{N_2}}{a\cdot D+2D_{N_2}}\right)\cdot\frac{b}{(a\cdot D+D_{N_2})^3}\cdot\frac{(D+D_{He})^3}{D^3}$$

Model 2 – correlation equations, cntd.

(i) *Corrected* for the cross-sectional area of N_2

$$S\,[m^2/g] = \left(1 - \frac{3 \cdot D_{N_2}}{D + 2D_{N_2}}\right) \cdot \frac{728.36}{(D + D_{N_2})} \cdot \frac{(D + D_{He})^3}{D^3}$$

a – relaxed variable
(relaxed D)

$$S\,[m^2/g] = \left(1 - \frac{3 \cdot D_{N_2}}{a \cdot D + 2D_{N_2}}\right) \cdot \frac{728.36}{a \cdot D + D_{N_2}} \cdot \frac{(D + D_{He})^3}{D^3}$$

a, b – relaxed variables
(relaxed D and one "constant")

$$S\,[m^2/g] = \left(1 - \frac{3 \cdot D_{N_2}}{a \cdot D + 2D_{N_2}}\right) \cdot \frac{b}{a \cdot D + D_{N_2}} \cdot \frac{(D + D_{He})^3}{D^3}$$

a, b, c – relaxed variables
(relaxed D and two "constants")

$$S\,[m^2/g] = \left(1 - \frac{c \cdot D_{N_2}}{a \cdot D + 2D_{N_2}}\right) \cdot \frac{b}{a \cdot D + D_{N_2}} \cdot \frac{(D + D_{He})^3}{D^3}$$

Model 3 – correlation equations

(i) *No correction* for the cross-sectional area of N_2

$$S\,[m^2/g] = \left(1 - \frac{6 \cdot D_{N_2}}{D + 2D_{N_2}}\right) \cdot \frac{728.36}{D} \cdot \frac{(D + D_{He})^3}{D^3}$$

a – relaxed variable
(relaxed D)

$$S\,[m^2/g] = \left(1 - \frac{6 \cdot D_{N_2}}{a \cdot D + 2D_{N_2}}\right) \cdot \frac{728.36}{a \cdot D} \cdot \frac{(D + D_{He})^3}{D^3}$$

a, b – relaxed variables
(relaxed D and one "constant")

$$S\,[m^2/g] = \left(1 - \frac{6 \cdot D_{N_2}}{a \cdot D + 2D_{N_2}}\right) \cdot \frac{b}{a \cdot D} \cdot \frac{(D + D_{He})^3}{D^3}$$

a, b, c – relaxed variables
(relaxed D and two "constants")

$$S\,[m^2/g] = \left(1 - \frac{c \cdot D_{N_2}}{a \cdot D + 2D_{N_2}}\right) \cdot \frac{b}{a \cdot D} \cdot \frac{(D + D_{He})^3}{D^3}$$

Model 3 – correlation equations, cntd.

(i) *Corrected* for the cross-sectional area of N_2

$$S\,[m^2/g] = \left(1 - \frac{6 \cdot D_{N_2}}{D + 2D_{N_2}}\right) \cdot \frac{728.36 \cdot (D + D_{N_2})^2}{D^3} \cdot \frac{(D + D_{He})^3}{D^3}$$

a – relaxed variable
(relaxed D)

$$S\,[m^2/g] = \left(1 - \frac{6 \cdot D_{N_2}}{a \cdot D + 2D_{N_2}}\right) \cdot \frac{728.36 \cdot (a \cdot D + D_{N_2})^2}{(a \cdot D)^3} \cdot \frac{(D + D_{He})^3}{D^3}$$

a, b – relaxed variables
(relaxed D and one "constant")

$$S\,[m^2/g] = \left(1 - \frac{6 \cdot D_{N_2}}{a \cdot D + 2D_{N_2}}\right) \cdot \frac{b(a \cdot D + D_{N_2})^2}{(a \cdot D)^3} \cdot \frac{(D + D_{He})^3}{D^3}$$

a, b, c – relaxed variables
(relaxed D and two "constants")

$$S\,[m^2/g] = \left(1 - \frac{c \cdot D_{N_2}}{a \cdot D + 2D_{N_2}}\right) \cdot \frac{b(a \cdot D + D_{N_2})^2}{(a \cdot D)^3} \cdot \frac{(D + D_{He})^3}{D^3}$$

Correlation coefficients

CORRELATION COEFFICIENT R a,b,c – adjusted constant(s) in the fitted model equations									
Model 1 (double adsorbate layer particle bridging)									
Correction for cross-sectional area of N_2	BET			LANGMUIR			BJH		
	a	a,b	a,b,c	a	a,b	a,b,c	a	a,b	a,b,c
Yes	0.84	0.94	*n/a*	0.87	0.92	*n/a*	0	0.64	*n/a*
No	0.91	0.95	*n/a*	0.87	0.94	n/a	0.64	0.76	*n/a*
Model 2 (single adsorbate layer particle bridging)									
Correction for cross-sectional area of N_2	BET			LANGMUIR			BJH		
	a	a,b	a,b,c	a	a,b	a,b,c	a	a,b	a,b,c
Yes	0.65	0.95	0.93	0.95	0.95	0.92	0.55	0.86	0.90
No	0.95	0.95	0.95	0.80	0.95	0.95	0.82	0.82	0.80
Model 3 (no adsorbate layer particle bridging)									
Correction for cross-sectional area of N_2	BET			LANGMUIR			BJH		
	a	a,b	a,b,c	a	a,b	a,b,c	a	a,b	a,b,c
Yes	0.94	0.95	0.95	0.73	0.95	0.95	0.88	0.89	0.90
No	0.88	0.95	0.95	0.56	0.95	0.95	0.81	0.90	0.90

Model 1 – selected best fits for BET, Langmuir, and BJH data

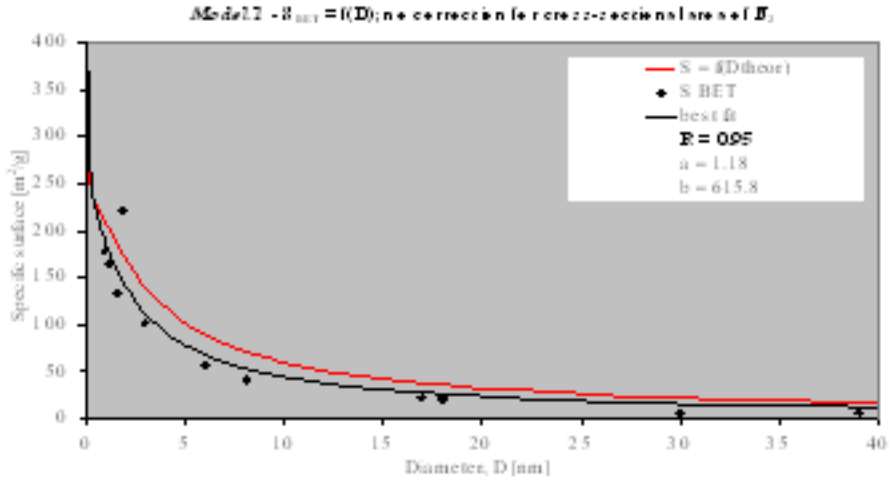

(i) very good overall fits for the BET and Langmuir data, a rather bad fit for the BJH data

(ii) distinct characteristics of the $S_{BJH} = f(D)$ relationship for D < *ca.* 5 nm
- not compatible with Model 1

(iii) uncertainty in the trend for D < *ca.* 2-3 nm
- *what are nano-GaN low size limits?*

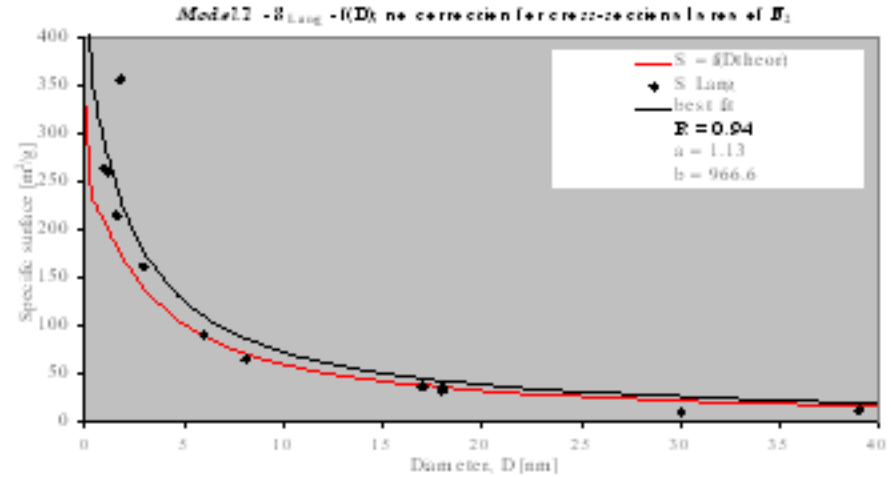

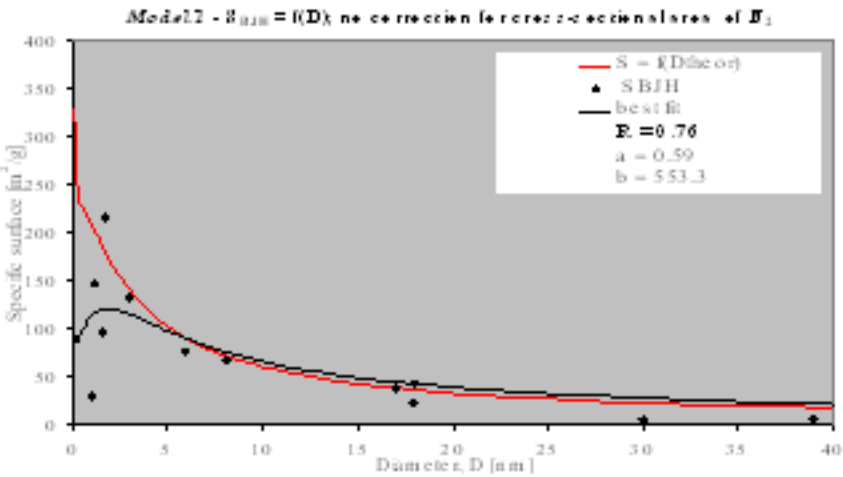

Model 2 – selected best fits for BET, Langmuir, and BJH data

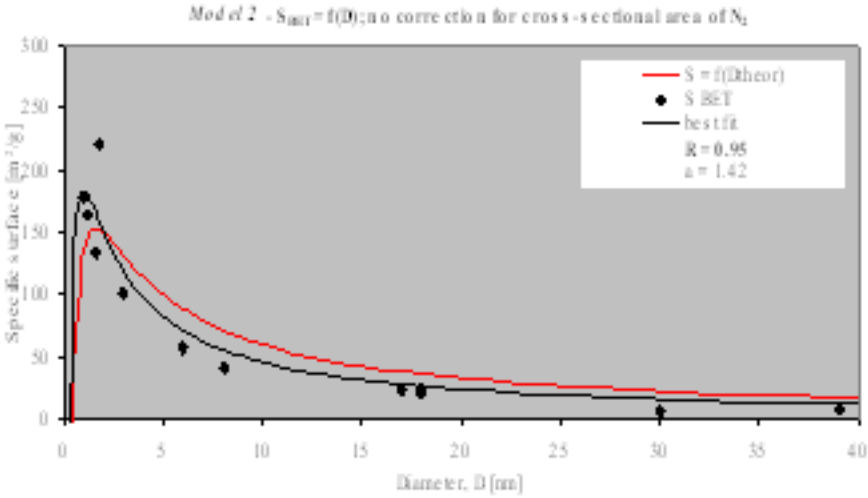

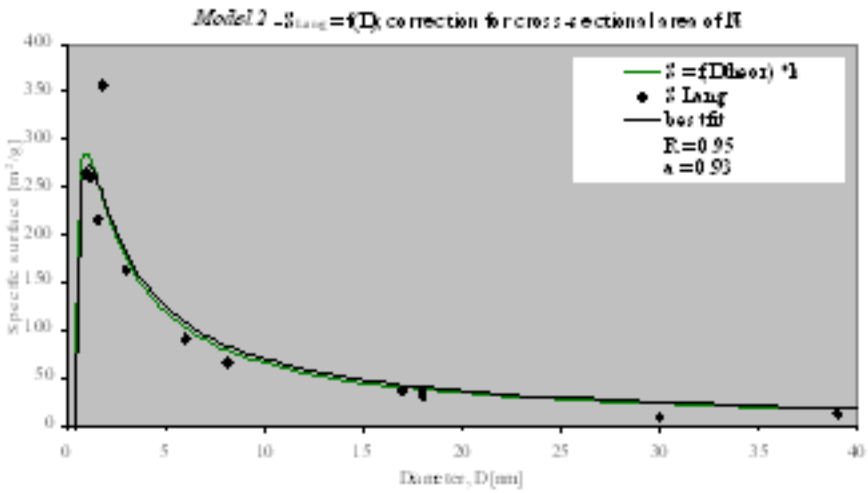

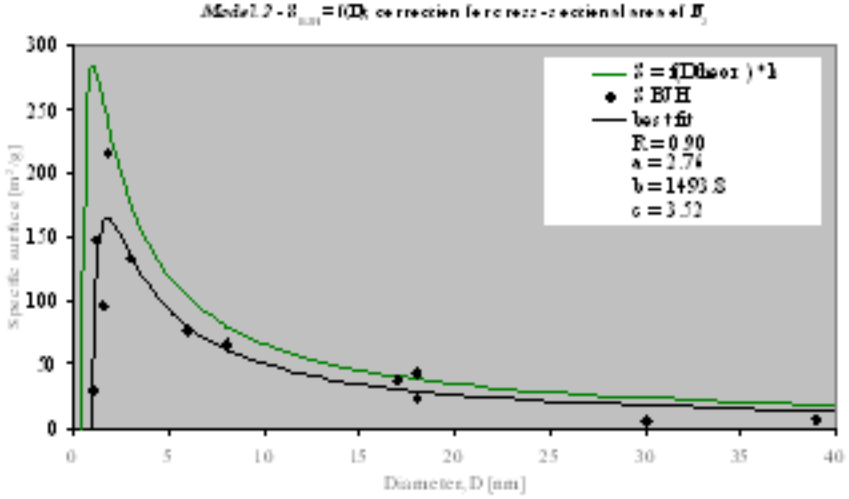

(i) very good overall fits for the BET and Langmuir data, and a good fit for the BJH data

(ii) similar relationship characteristics suggested for all data (local maxima in the smallest D range)

(iii) correction for the cross-sectional area of N_2 beneficial for the BJH data fit

(iv) small spread between the model curves (red or green) and the best fit curves (black)

Model 3 – selected best fits for BET, Langmuir, and BJH data

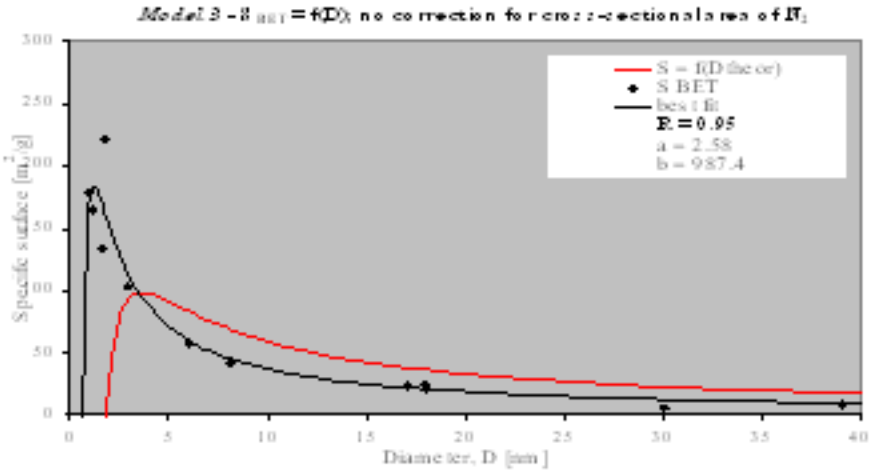

(i) very good overall fits for the BET and Langmuir data, and a good fit for the BJH data

(ii) similar relationship characteristics suggested for all data (local maxima in the smallest D range)

(iii) relatively large spread between the model curves (red) and the best fit curves (black)

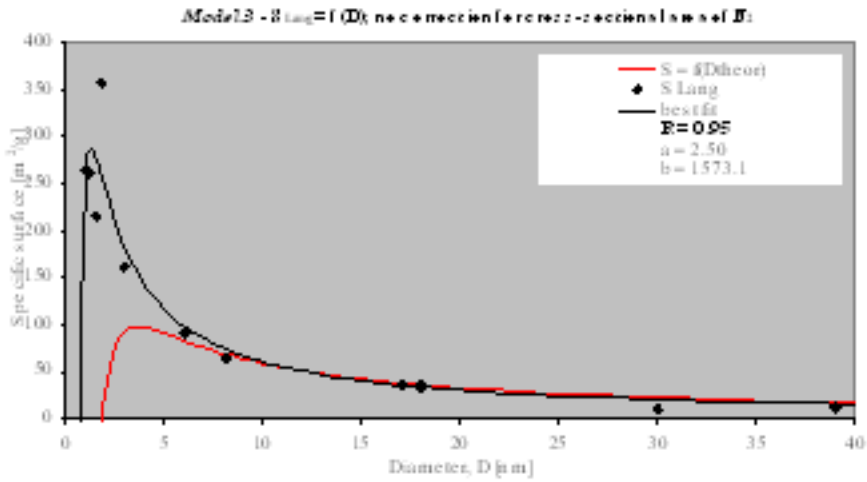

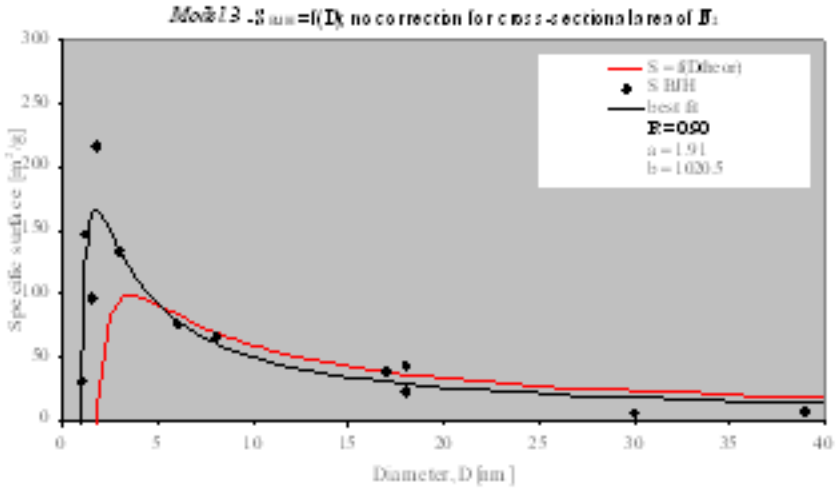

Conclusions

1. A pool of twelve GaN nanopowders with crystallite sizes spanning the 1 to 40 nm range (from powder XRD scans) was shown each to consist of *tight agglomerates of regularly shaped crystallites forming larger loose aggregates* as supported by characteristic size dependent helium densities and SEM/TEM examinations.

2. A general model of porosity of such nanopowders was proposed wherein the *pore system and pore surface area could be represented by the interparticle spaces and surface area, respectively, of closely packed equiradial spherical agglomerates of particles*:

   (i) three cases of the model were investigated, namely, Model 1 – with double adsorbate layer particle bridging, Model 2 – with single adorbate layer particle bridging, and Model 3 – with no adsorbate layer particle bridging; all model equations for S = f(D) were derived with the option to include corrections for the sphere curvature adjusted cross-sectional area of the adsorbate molecule,

   (ii) within the limits of the smallest particle sizes going from *ca.* 5 to 1 nm, Model 1 predicted steeply increased surface areas with values reaching a few hundred m^2/g while Model 2 and Model 3 suggested local maxima of lower magnitude for the diameters of *ca.* 1-2 nm and 3-4 nm, respectively.

Conclusions, cntd.

3. The model-based relationships of the surface area as function of sphere diameter, now with some relaxed variables, were statistically fitted for the cases of the BET, Langmuir, and BJH surface areas (from low temperature nitrogen adsorption experiments) being a function of the average crystallite size (from powder XRD scans):

   (i) the best fits for the BET and Langmuir surface areas *vs.* D_{XRD} yielded for both the correlation coefficients R equal to 0.95 while for the BJH data R reached 0.90, *supporting the overall very good relevance of the applied models*,

   (ii) it appeared that the *circumstances somewhat between Model 1 and Model 2 are the closest to best describe the experimental data* as far as the magnitude of the particular surface area is concerned,

   (iii) it is our opinion that the observed discrepancies between the model and the experimental data in each case are, at least, partly due to the unknown degree of agglomeration of the GaN crystallites and its likely dependence on D_{XRD}; *a mismatch between the D_{aggl} and D_{XRD} causes the displacement of the experimental and model curves*.

Acknowledgement. Research supported by the Polish Ministry of Science and Higher Education/MNiSW, Grant No. N N 507 443534.

AGH University of Science and Technology
Krakow, Poland

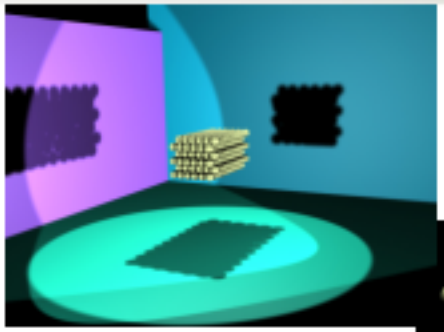

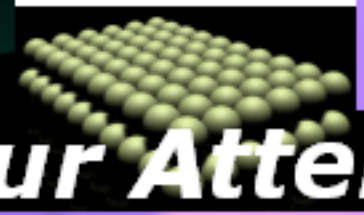

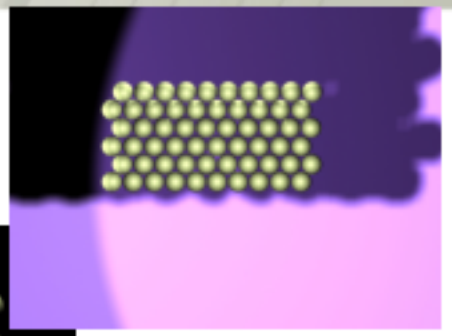

Thank You For Your Attention

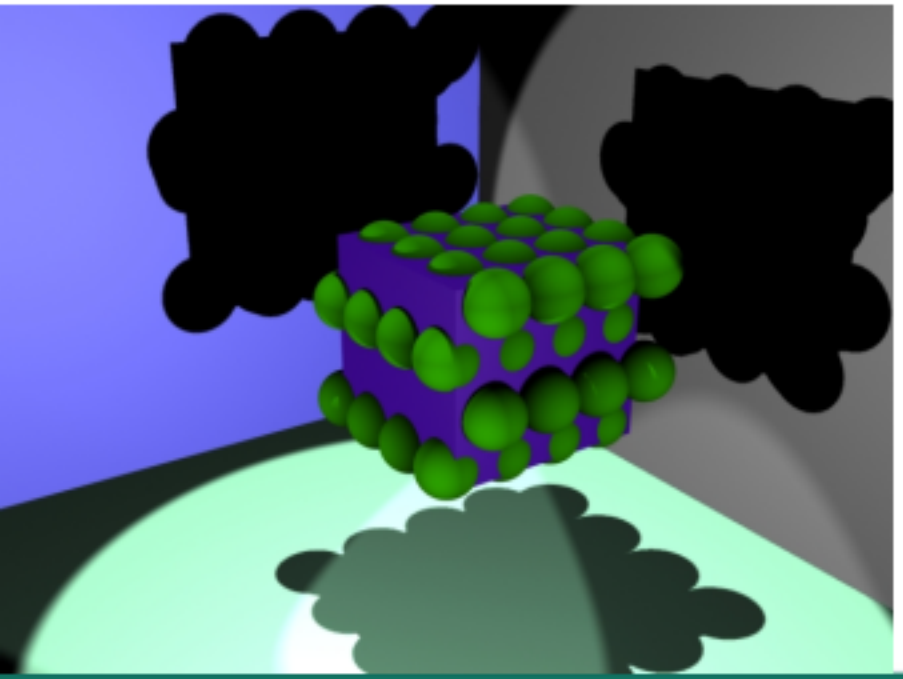

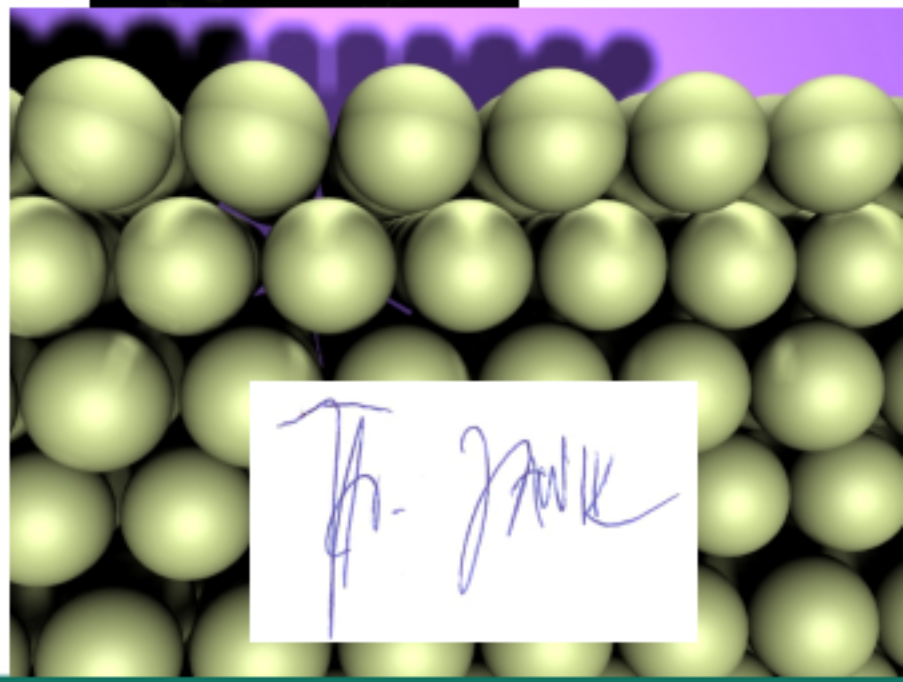

Appendix
Adsorption isotherms (N_2, 77.5 K) and mesopore distribution (BJH) - 1

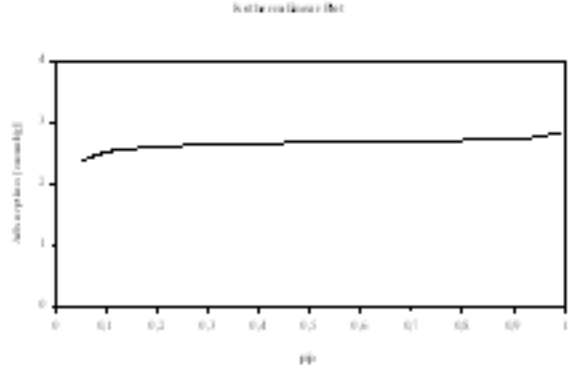

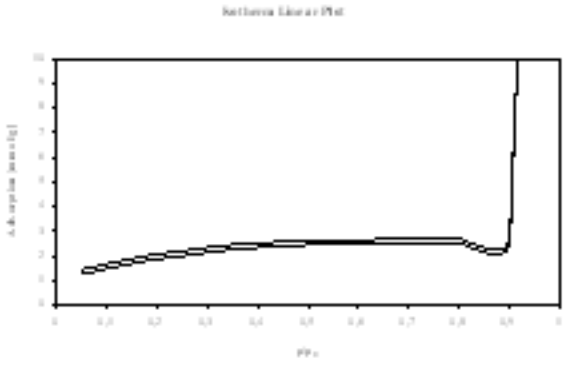

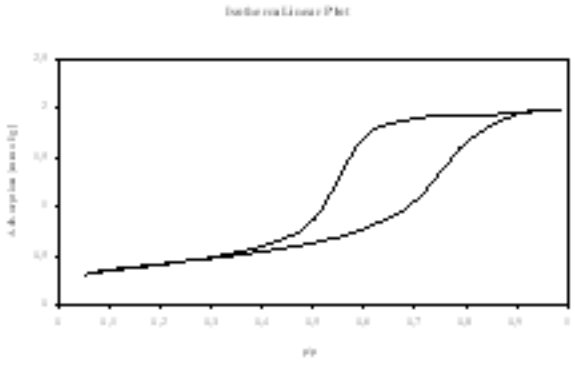

Anaero_450_vac

Anaero_450_N_2

Anaero_350_NH_3

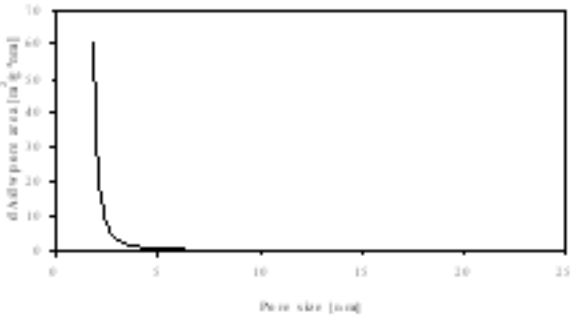

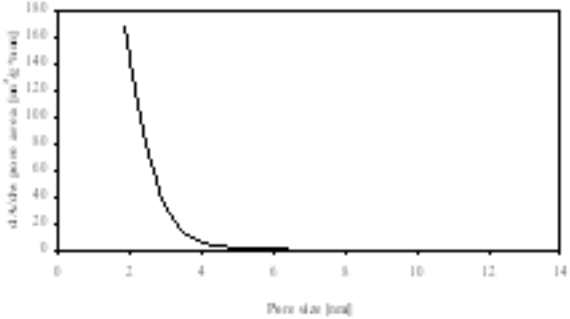

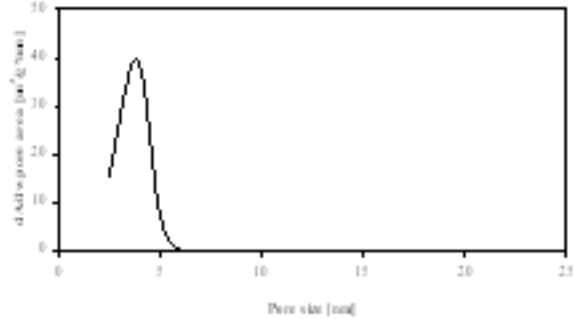

Appendix
Adsorption isotherms (N_2, 77.5 K) and mesopore distribution (BJH) - 2

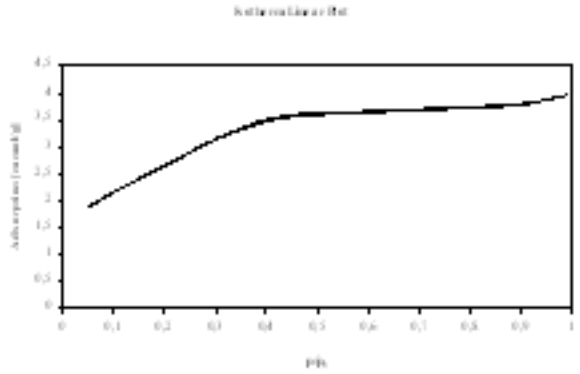

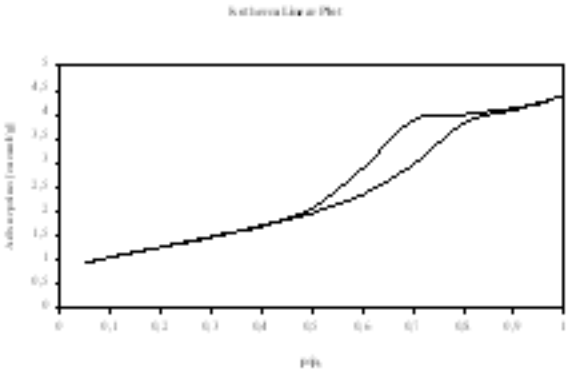

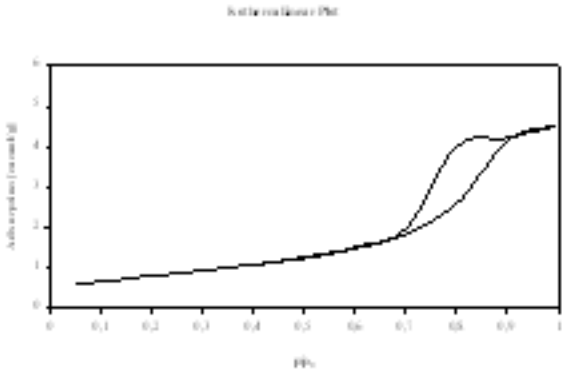

Anaero_450_NH_3

Anaero_600_NH_3

Anaero_700_NH_3

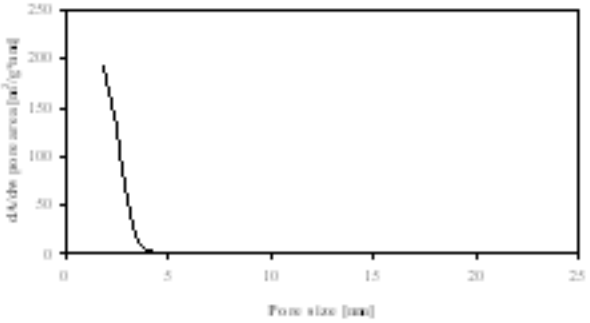

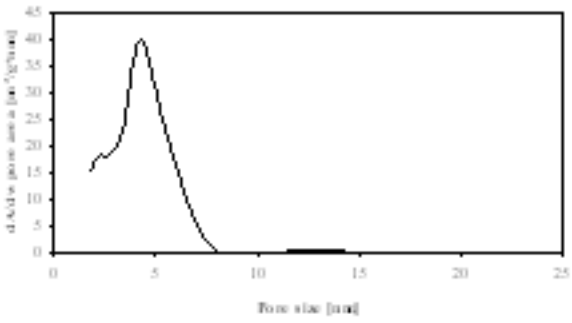

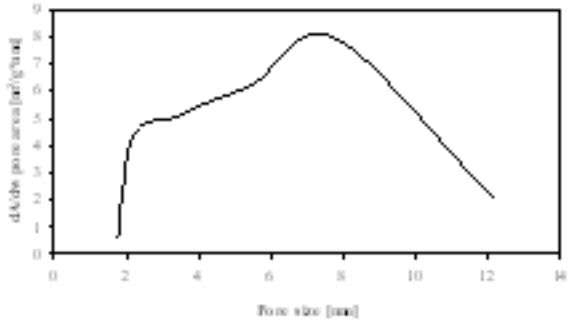

Appendix
Adsorption isotherms (N_2, 77.5 K) and mesopore distribution (BJH) - 3

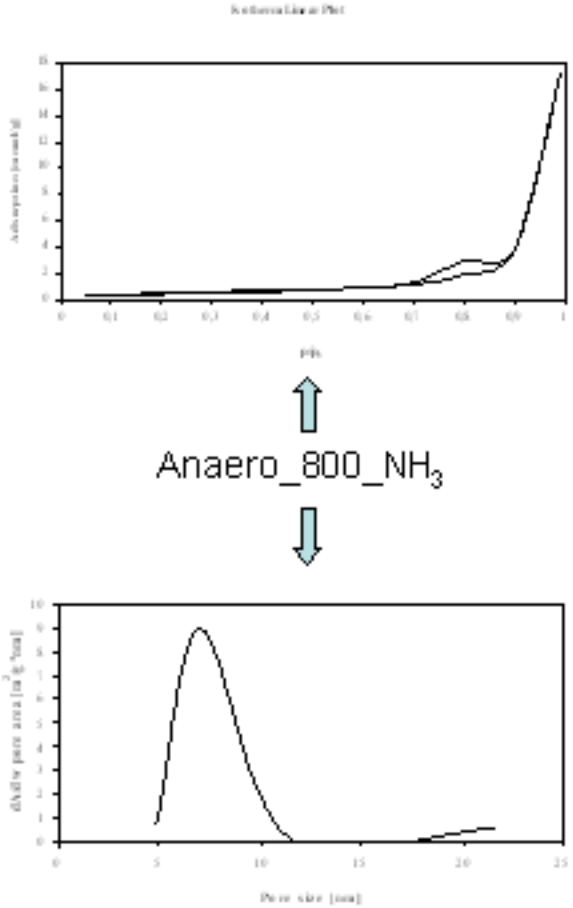

Anaero_800_NH_3

Appendix
Adsorption isotherms (N_2, 77.5 K) and mesopore distribution (BJH) - 4

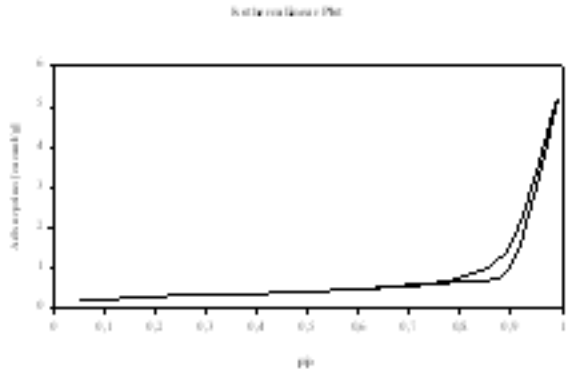

Aero_DMF/MeOH_950

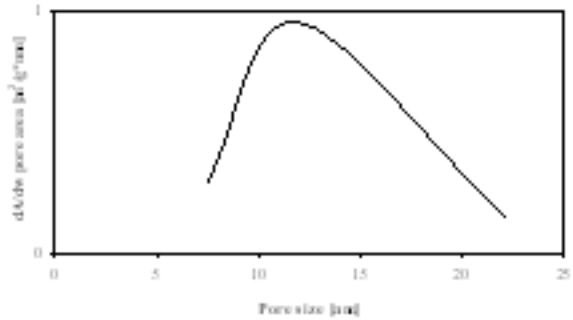

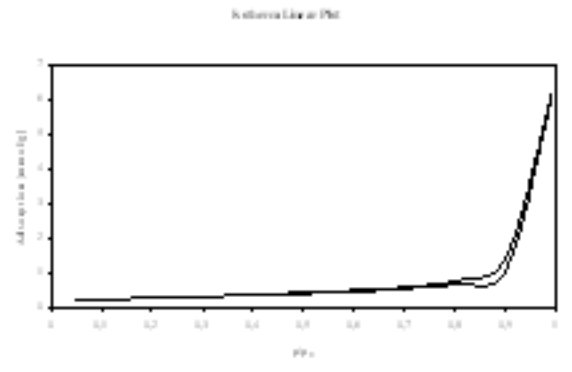

Aero_DMF_950

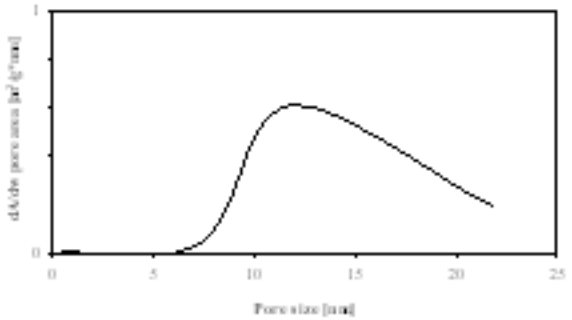

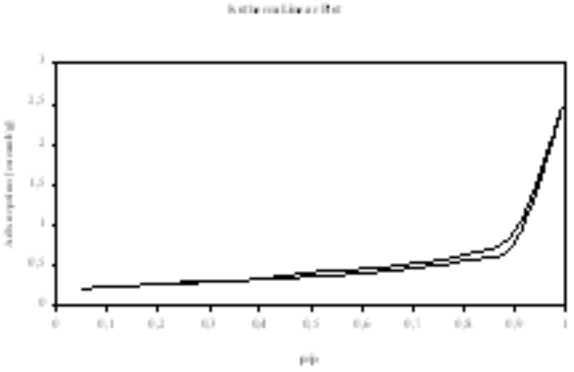

Aero_MeOH_950

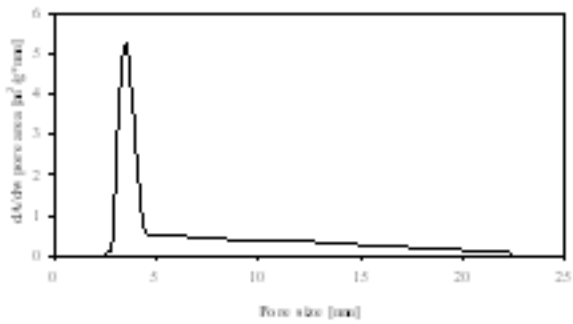

Appendix
Adsorption isotherms (N_2, 77.5 K) and mesopore distribution (BJH) - 5

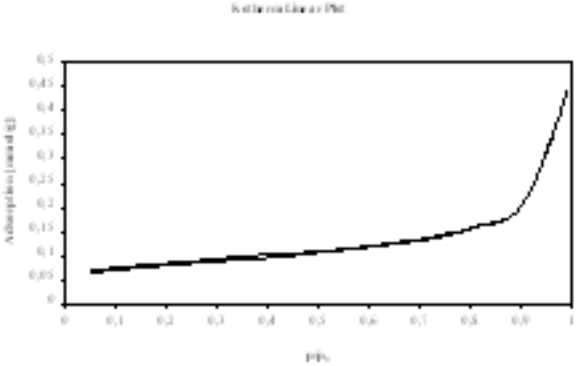

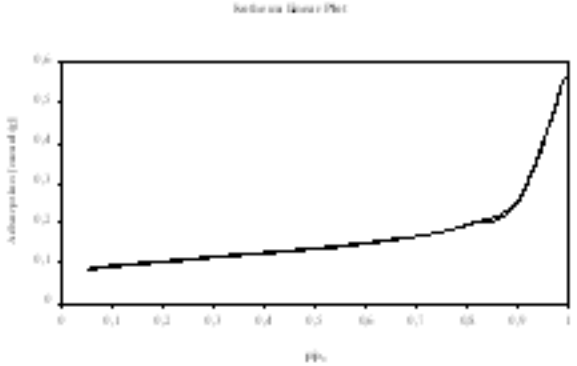

Aero_H_2O_975

Ga_2O_3_950

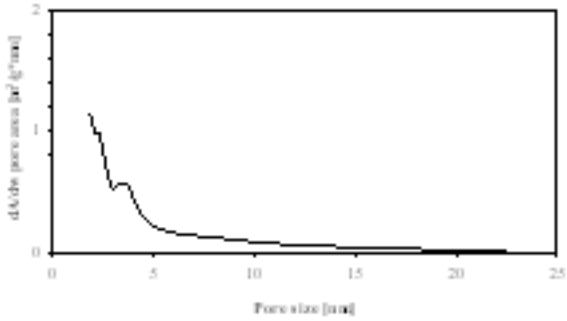

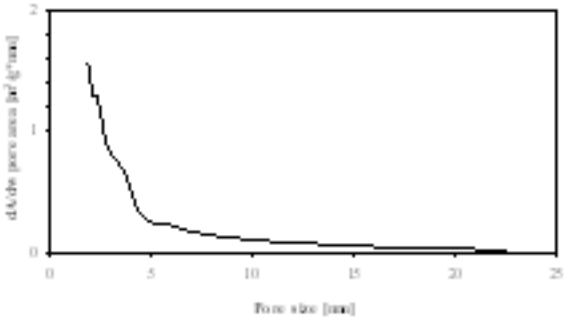

Appendix
Langmuir theory - 1

Assumptions of Langmuir theory

http://upload.wikimedia.org/wikipedia/commons/0/0b/Langmuir_izoterma.png

1. Fixed number of adsorption sites are available on the surface.
2. All the vacant sites are of equal size and shape on the surface.
3. Each site can hold maximum of one gaseous molecule and a constant amount of heat energy is released during this process.
4. Dynamic equilibrium exists between adsorbed gaseous molecules and the free gaseous molecules.

$$A(g) + B(s) \underset{\text{desorption}}{\overset{\text{adsorption}}{\rightleftharpoons}} AB$$

5. Adsorption is monolayer.

Appendix
Langmuir theory - 2

Langmuir adsorption equation in terms of pressure P:

$$\frac{P}{V} = \frac{P}{V_{mono}} + \frac{1}{KV_{mono}}$$

If we plot a graph between P/V vs. P, we will obtain a straight line with

$$\text{slope} = \frac{1}{V_{mono}} \quad and \quad \text{intercept} = \frac{1}{KV_{mono}}$$

V_{mono} - adsorbed volume of gas covering the surface with a monolayer

K – constant; $K = \frac{K_a}{K_d}$; K_a – rate of adsorption, K_d – rate of desorption

Appendix
Brunauer, Emmett, Teller (BET) theory -1

Assumptions of BET theory

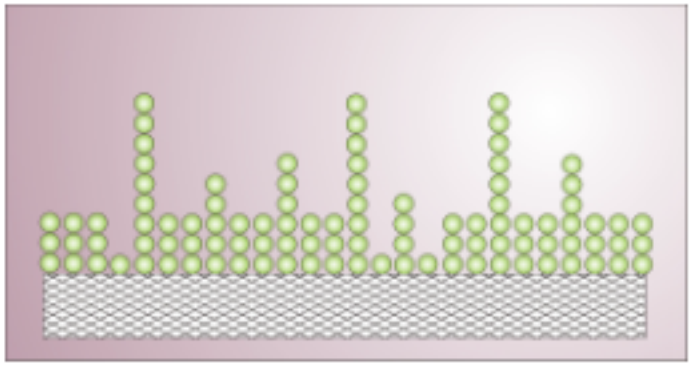

http://upload.wikimedia.org/wikipedia/commons/8/83/BET_Multilayer_Adsorption.jpg

The concept of the theory is an extension of the Langmuir theory, which is a theory for monolayer molecular adsorption, to multilayer adsorption with the following hypotheses.

1. Gas molecules physically adsorb on the surface with random distribution of sites covered by one, two, three, etc. molecules.
2. There is no interaction between each adsorption layer.
3. The Langmuir theory can be applied to each layer.

Appendix
BET theory - 2

Classical form of the BET equation:

$$a = a_m \cdot \frac{Ch}{(1-h)[1+(C-1)h]}$$

where:

a - the adsorption capacity equilibrium humidity h
h - the relative pressure ($h = p/p_s$)
p - the equilibrium partial pressure of the adsorbate vapor
p_s - the saturated vapor pressure of the adsorbate at absolute temperature T
a_m - monolayer capacity
C - energy constant:

$$C \approx \exp[-(E_1 - E_L)/RT]$$

E_1 - heat effect of adsorption in the first layer
E_L - latent heat of condensation
R - the gas constant

- the coordinates of the points of monolayer h_m calculated according to the known formula:

$$h_m = 1/(\sqrt{C}+1)$$

- the first layer heat of adsorption calculated from the equation:

$$E_1 - E_L = RT\ln(C)$$

where: - E_1 is the first layer heat of adsorption, E_L is the heat of condensation, R is the gas constant, and T is the absolute temperature,
- surface area of samples calculated from a_m values assuming that cross-sectional area of adsorbed nitrogen molecule is 0.162 nm^2.

Appendix
Barrett, Joyner, Halenda (BJH) theory

Assumptions of BJH theory

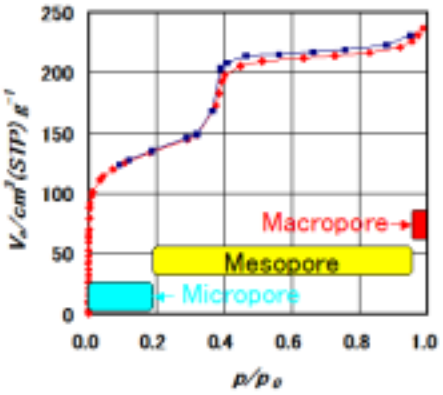

1. The relative pressure p/p_o at which decondensation (from capillary phase to multilayer adsorbed phase) occurs in a cylindrical pore is given by the Kelvin law.

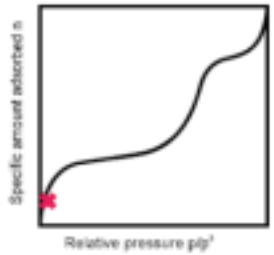

$$kT\ln(p/p_o) = -2\,\sigma\,v_l/(R-t)$$

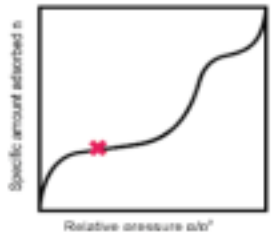

k – Boltzmann constant, T – temperature, p – equilibrium pressure, p_o – saturation vapor pressure, σ – surface tension, v_l – liquid molecular volume, R – pore radius, t – multilayer thickness

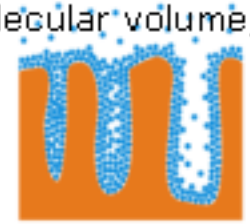

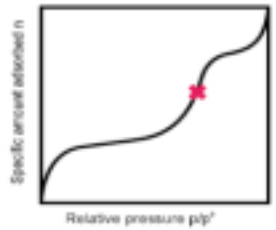

2. The curvature of the solid surface has no influence on *t*. Thus, *t* can be experimentally determined using non porous adsorbents.

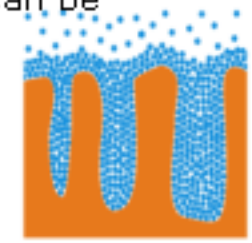

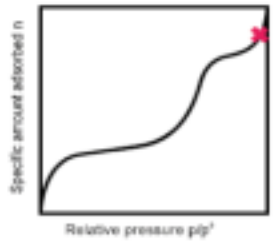

$$kT\ln(p/p_o) = U(t)$$